V-KEMS Report

COVID19 Safety in Large Events

WARNING: this report contains preliminary findings that have not been peer reviewed. The findings are intended to provoke further study and policy discussion and should not be treated as definitive scientific advice in response to the SARS-CoV-2 epidemic.

Whilst we expect these principles to help others formulate coherent and consistent guidelines, time has prevented any quantitative study of their effectiveness. This could be undertaken, but would require real data and time to build more detailed simulation tools. Thus, we are not able to make specific recommendations from the principles, e.g. we cannot infer that it is safe to do X if you follow principle Y.

Additionally, this report has been assembled in a short time frame, we have made every effort to ensure references and links are present. Where this is not the case, we apologies for the unintentional oversight.

Contents

1   Executive Sumary

The events industry in the UK is a major contributor to GDP. The Business Visits & Events Partnership (BVEP) estimates the value to the economy (pre-COVID19) at £70 billion. In addition, the industry provides 700,000 jobs [1].

A business survey conducted in Aug 2020 [2], reported that due to a significant reduction in demand for events due to the pandemic, 40 % of all those surveyed suggested that the business they are involved in may not exist in its current form within the next 6 - 12 months and urged that alterations to the realignment of their costs are imperative in order to stay afloat.

The UK Government (BEIS, DHSC, and DCMS) in mid 2021 led the he Events Research Programme (ERP) [3]. ERP aimed to examine the risk of transmission of COVID19 from attendance at events and explore ways to enable people to attend a range of events safely. To achieve this, the ERP explored how a combination of testing and non-pharmaceutical interventions (NPIs) can inform decisions on safely lifting restrictions at events. This was run primarily through the delivery of a pilot programme of large events.

Guidance was published by the UK Government [4] prior to the general unlocking of restriction on the 19th July 2021. There are still hard questions for the industry (and in particular, individual organisers) to consider, and how might they translate this guidance into their particular settings?

In July 2021, the International Centre for Mathematical Sciences (ICMS) held a three day Virtual Study Group (VSG) which bought together around 40 university researchers and events experts to consider topics which mathematical modelling could provide insight into. For the purposes of the VSG, the group considered topics in; indoor events, outdoor (ticketed), and outdoor (unticketed).

The organisers are grateful to all those list in the contributors listed in previously. In particular, we would like to thank ASM Global, Edinburgh Fringe Festival, Church of England and Bath Rugby Club for enlightening discussion. In addition, the VSG was fortunate to have received input from experts on topics such as crowd psychology, test & trace, events management, viral load dynamics. The VSG thanks them also for their contributions.

---

[1] https://www.businessvisitsandeventspartnership.com/news/bvep-press-releases/801-bvep-launches-report-focused-on-70bn-events-industry

[2] https://www.eventindustrynews.com/news/covid-19-business-impact-study-global-perspective

[3] https://www.gov.uk/government/publications/information-on-the-events-research-programme/information-on-the-events-research-programme

[4] https://www.gov.uk/guidance/working-safely-during-covid-19/events-and-attractions

- **Indoor events**

  1. the **queuing** section considers how arrival profiles, and queuing designs can be modelled so as to minimise the risk of exposure where queuing is necessary. We tentatively suggest that designing queues in longer, fewer rows could reduce the number of individuals at risk from COVID19. Future work might consider more realistic social groupings for arrivals and suggest the use of events data to paramaterise the model.

  2. the **testing** section seeks to address the incoming viral load at a venue with a number of occupants given some pre-screening regime through lateral flow devices. This estimated load could be used to inform models which calculate risk from aerosol spread. the proof of principle shows how this could be done with more time, and suggests the integration of data around age demographic, prevalence, variant types etc.)

  3. the **ventilation** section considers how mathematical modelling can provide a framework to optimise the placement of ventilation to minimise the virus concentration in a room containing a number of people, some infectious. A draft formulation is presented, but has not been simulated.

- **Outside & ticketed events.**

  1. considering the **arrival** at the venue, a model to rationalise seat allocation (based on vaccination status) is introduced. The impact of this approach suggests a minimal effect on transmission risk. Queuing types are considered to demonstrate the impact of pre-checking, arrival profiles etc. Pre-checking is shown to be useful in reducing the waiting time if temperature checks are required.

  2. mitigation effects **in stadium** are modelled considering the journey of uncontrolled event attendees to bars situated around a stadium interior. The interaction of the agents is modelled by way of the contacts made. During breaks, visitors should be encouraged to go to the bar at different times as this can reduce the transmission risk. The effective use of signage to reduce confusion is explored and suggests this is another useful mitigation factor.

- **Outside & unticketed events.**

  1. the **person-to-person modelling** derives an approximation which provides a 'quanta of infection' which allows for simple, diffusion type modelling on how virus dissipates for use in the rest of the section.

2. the **audience modelling** section uses a lattice based model to simulate movement of individuals in an open space over time whilst watching a street performer. The relative impact of wearing a mask in an audience compared with shortening the show is considered. A tentative conclusion is that mask wearing during a performance is the most effective measure to reduce risk.

3. the **crowd dynamics** section considers how dynamic crowd measures (such as redirection) could be used to minimise congestion of crowds (therefore infection of risk). Future work would need to consider a more sophisticated behavioural understanding of these crowds.

2 Indoors

This section considers topics of importance to hosting large event in indoor settings. In particular, this section discusses the role of **queue design, testing regimes and ventilation optimisation** on possible COVID19 risk.

2.1 Can we control the length and geometry of a queue to minimise infection risk?

Aim: Here we consider people arriving to a ticketed event. Upon arrival individuals have their tickets and SARS-CoV-2 test results checked. This is likely to cause a queue. Large venues may have multiple 'gates' in which people enter. Here we consider one 'gate', however the model could be for each gate to allow for heterogeneities in footfall. We examine two event management techniques for potentially minimising attendees' risk of exposure of SARS-CoV-2 whilst queuing to enter an event. Firstly, we analyse the potential of having tickets with 'time slots' for entry. This method is an attempt to minimise the number of people in the queue in order for social distancing to be maintained. We also consider the geometry of the queue design. We access three types of risk:

1. Risk to attendees to other attendees in the queue.

2. Risk to attendees from an infected ticketer.

3. Risk to ticketer from infected attendees.

2.1.1 Methods

Queue Positions: The following schematic describes the basic design of our model. We have individuals entering a ticket queue waiting to be served by one of multiple ticketers.
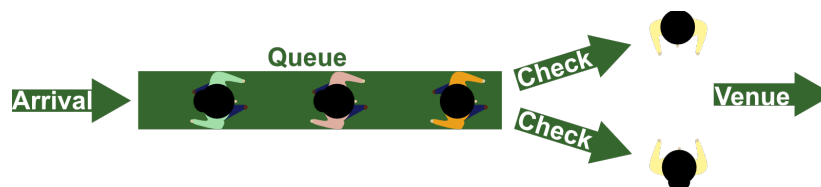
There are two possible events which change the positions of individuals in the queue:

- **Arrival** - Individuals are given a time to arrive. This could be one time or multiple slots. People arrive according to a normal distribution around their given time slot.

- **Exit** - Individuals leave the queue according to the length of time taken to check their ticket. This is modelled by a Cauchy distribution. This distribution (shown below) can be given a minimum / maximum to make it more realistic.
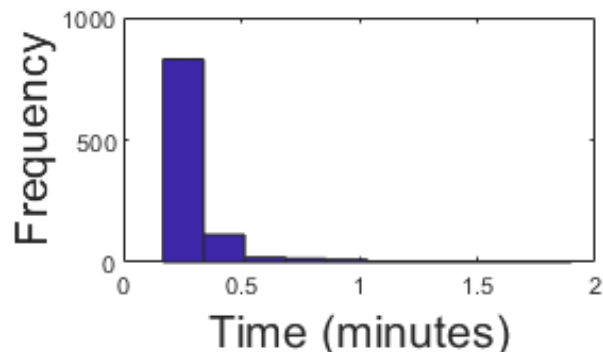
Our model uses a stochastic time-step which is the time until the next arrival or exit.

Spatial layout: We explore different queue geometries inspired by the findings of Ref. [4]. Within our work, we compare the effects of having many short rows or fewer long rows on the number of individuals exposed to SARS-CoV-2.
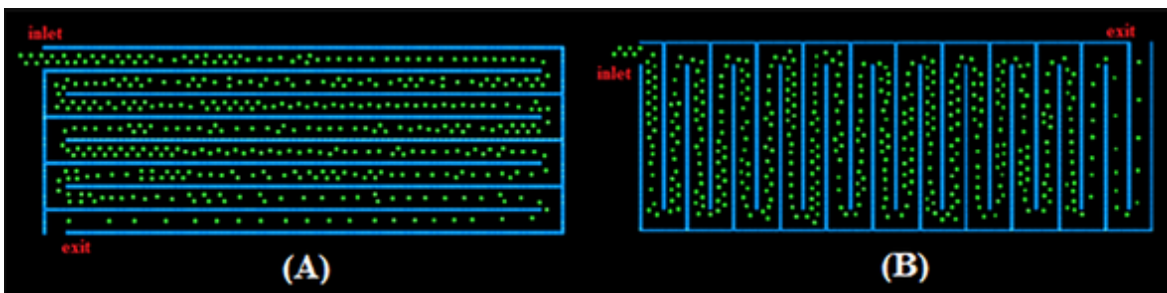
Figure 1: Image source, Ref. [4]

We assume individuals in the queue socially distance where possible, but if the queue is busy, then they may not. Therefore if the queue is not 'full' we simplify the pedestrian dynamics suggested in Ref. [4], assuming a lattice model where all the individuals stay a fixed distance $d = 2$ m apart.

Viral spreading: Individuals are assigned a positive or negative SARS-CoV-2 status dependent on the expected proportion of positive individuals. Given N individuals attend an event, if the proportion in infected individuals was estimated to be p, a binomial distribution of N trials and

probability p is used to determine the number of positive cases. This method is also used to assign ticketers as positive.

Each time-step the positions of individuals in the queue changes. Therefore, we calculate the x and y coordinates for each individual each time step. The euclidean distance between infected individuals and others is then calculated. The distance from an infected individual and the duration of the time step are then used to calculate the 'viral dose' received. The cumulative viral dose from each infected individual at each time step is then used to estimate the risk of infection. When modelling the airborne viral spread we follow the approach in Ref. [6]. For each susceptible individual i we compute the cumulative viral dose

$$Q_i = \sum_{j \in \text{'infectious'}} \int \frac{\alpha}{|\vec{x_i}(t) - \vec{x_j}(t)|^2} dt,$$

where $\vec{x}_i$ is the spatial position of individual i and it is understood that the transmission occurs if and only if both i and j are present in the queue. Note that we assume that equal emission strength α for all the infectious people, but in a more realistic model it could be modelled as a random variable.

The units of Q are emission quanta (EQ) [5]. For simplicity, we fix $\alpha = 16[\text{EQ}]\text{m}^2\text{h}^{-1}$ and we assume that an individual is at a significant risk if $Q > 1$ EQ. This estimate is based on some back-of-envelope calculations (note that $Q = 1$ EQ corresponds to 15 minutes spent 2m away from an infectious person), but in a future work a more careful treatment would be desirable (see Ref. ???). We estimated the risk from an infected ticketer to an attendee by assuming that the queuer stands 0.5m from the ticketer while being served.

Parameters: The following parameters are needed to run our model. We assign default values, but note that venue / event-specific information is required.

Table 1: Parameters for queuing model.

Parameter	Definition	Values
N	people going into gate	900
Groups	No. of time slots	1:10
TicketRate	Mean time taken to process ticket (minutes)	15/60
TicketRateScale	Cauchy scale parameter for processing ticket time	0.05
minTicketRate	Minimum ticket processing time (minutes)	10/60
maxTicketRate	Maximum ticket processing time (minutes)	2
Ticketers	No. of ticket processors	4
OpenEarly	Venue opens x minutes before first ticket time	15

Start	Time before event of first ticket	60
ArrivalSd	Arrival standard deviation	15
Prevalence	Percentage of people we expect to be positive	0.02
N_QueueRows	Number of rows in the queue	-
N_QueueRowLength	Length of each row in the queue	-

2.1.2 Results

Queue length: Fig. 2 (left) shows the average time spent in the queue according to the number of distinct time slots / groups that we allocate. This shows that more time slots result in individuals spending less time in the queue. With those venues with limited space in mind, Fig. 2 (right) shows the maximum number of people in the queue given a number of distinct time slots / groups.
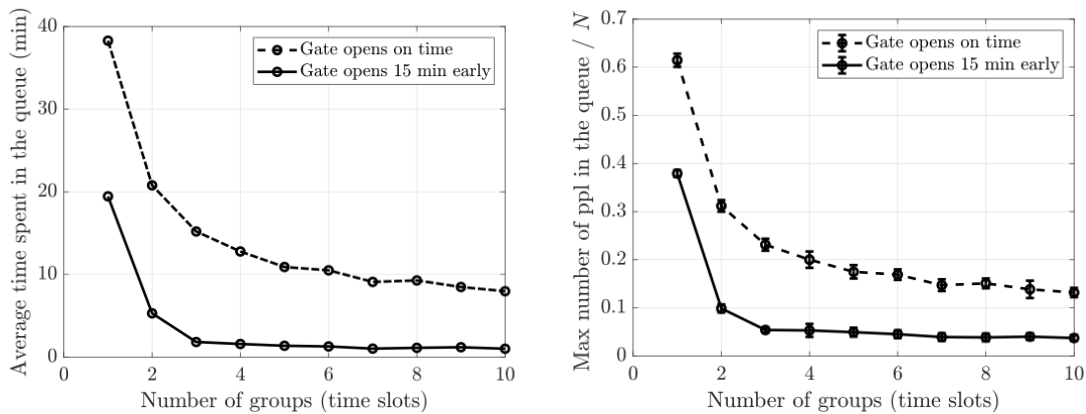
Figure 2: (left) Average time spent in queue according to the number of distinct time slots allocated. (Right) Maximum number of people in the queue given a number of distinct time slots.

Queue design:

The black dot in Fig. 3 represents an infectious individual and the grey dots represent people at (highest) risk. Unsurprisingly, the most exposed individuals are the immediate neighbours of the infected agent. Less obviously, the second most vulnerable group are the people two rows away. Indeed, their motion is by design correlated with the motion of the infected individual. Therefore, their cumulative viral dose is likely to be higher than the viral dose absorbed by the people one row away, who come into close contact with the infectious person only periodically. This observation suggests that the overall risk may be mitigated by choosing a partic-
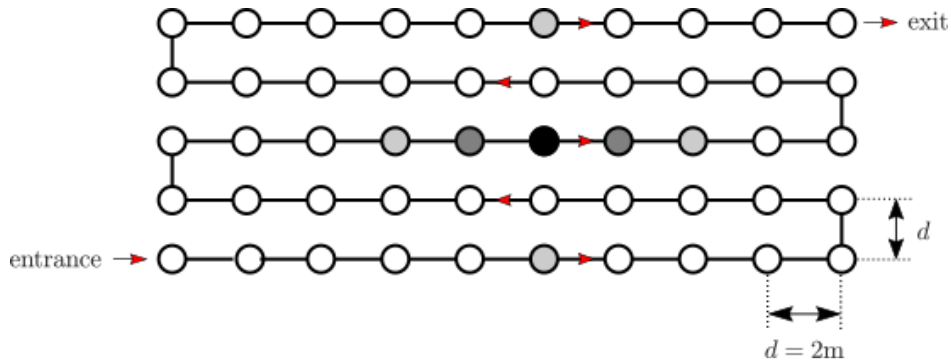
Figure 3: Example of a queue with $N = 50$ people with $n = 5$ 'rows' and $N/5 = 10$ people in each row.

ular shape of the 'queueing snake'. Fig. 4 shows the number of people at risk given a number of distinct time slots/groups for different queue designs.
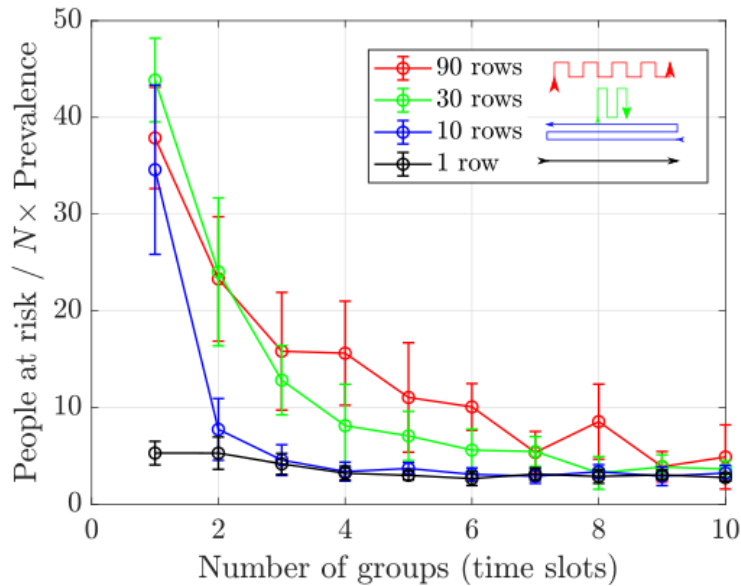
Figure 4: Number of people at risk given a number of distinct time slots for different queue designs.

This shows that the single file (1 row) solution is the best. This is to be expected as we do not have any cross-row spreading. Our simulations suggest also that the number of people at risk is usually reduced if the queue is arranged into a few long rows (as opposed to many short rows). This trend can be plausibly explained by thinking about the people one row away from the infectious individual. If the rows are short, they continually stay in the vicinity of the infectious individual. If the rows are long, they spend most of their time in the queue away from the source of infection (c.f. 'spatial layout' section).

Notably, [4] reach the opposite conclusion, i.e. they find that many short rows may reduce the

overall risk. One important difference is that in their simulation the motion of queuers is not strictly correlated. However, a comprehensive understanding of this discrepancy would require a much more thorough analysis.

2.1.3 Key findings

- The contributions to the cumulative 'viral dose' are generally much lower from infected ticketers apposed to infected attendees nearby in the queue. This is because queuers spend relatively little time with the ticketer.

- As each ticketer meets many people, this risk can rise to significant levels if the prevalence is high.

- Introducing multiple entry time slots may reduce the risk of SARS-CoV-2 infection of event attendees while queuing by reducing the number of individuals in the queue. In our simulations four time slots seem to significantly reduce risk. However, this may be parameter dependant.

- Our model suggests that fewer long rows reduce the number of individuals at risk of SARS-CoV-2 infection. However, this is likely to be dependant on the choice of cumulative 'viral dose' which determines whether an individual is at risk.

2.1.4 Caveats

- Here we conclude that an individual is 'at risk' if there cumulative risk is above a set value. However, the probability of infection is likely to increase with viral dose, with some people becoming infected with low levels of exposure to the virus.

- Our assumption that a critical viral load must be reached for an individual to become at risk of infection may underestimate the ability of an infected ticketer to transmit the virus to attendees. For an interaction to be dangerous the serving time would need to last almost a minute. The distribution of ticketing times means this is extremely rare within our model.

- Here we set the probability of an individual attending the event to 2%, however this is likely to be dependent on the demographic of the event and testing regimes prior to the event. Work from the testing group could therefore probably improve the accuracy of this estimate.

2.1.5 Future work

- Some individuals pay no attention to time slots.

- Un-ticketed event - This work could easily be adapted to model an unticketed event. Here the distribution of expected arrival times and time taken to process a ticket could be adapted to explain a different event type.

- Grouped attendees – Individuals may be more likely to arrive at an event in groups opposed to individuals. The size of the groups arriving could be assigned by the distribution of the number of tickets bought together.

- Many events will be recurring. We can improve our model for future events using data from prior events through the use of statistical inference.

2.2 Can we estimate the viral load at a venue given a certain testing regimes?

2.2.1 Venue viral load calculator

Aim: We estimate the incoming viral load at a venue with N occupants given pre-event screening with lateral flow device (LFD) tests for input into calculations for the expected transmission risk due to aerosolised virus [8].

Methods: We estimate the expected number of incoming infected individuals I in quanta of individuals at peak viral load of an unvaccinated symptomatic person Q.

$$I = n \cdot v \, Q,$$

where n is the vector of numbers of classes of people admitted to the event, and v is the vector of mean viral loads of those classes of people as a fraction of the peak viral load of an unvaccinated symptomatic person. We take the classes to be unvaccinated symptomatic, unvaccinated asymptomatic, single-vaccinated and double vaccinated people.

We calculate the number of people admitted in each class after lateral flow testing, using COVID19 prevalence rates in each class [9], test sensitivity data and viral load profiles over the days of infection [9] for the different classes. (Lateral flow testing can be switched off in the model.)

We include the impact of an exponentially growing or decaying epidemic (with up to 10% daily changing in the numbers of new infections) on the distribution of people in different stages of their infection, and hence on the likelihood that they will be screened out by testing.

$$n_i = r_i f_i L_i N,$$

where r is the vector of COVID19 prevalence [10], f is the vector of fractions of the population in each class estimated for England from [11; 12; 13], L is the vector of proportions of infected people who fail to be screened out by testing, and N is the total number of people attending the event.

Table 2: Prevalence and sensitivity estimates adopted. Note that the viral load defining the lateral flow test (LFT) sensitivity is marked in the figure below.

Parameter		Estimate	Source
Unvaccinated prevalence	r_u	1.16%	[10]
Single-vaccinated prevalence	r_1	0.82%	[10]
Double-vacccinated prevalence	r_2	0.33%	[10]
Low LFT sensitivity		10%	[14]
Medium LFT sensitivity		60%	[14]
High LFT sensitivity		90%	[14]
Proportion unvaccinated asymptomatic	f_a	0.3	[13]
Duration of infection		15 days	

We assume piecewise linear viral load profiles over the course of infection following [9]. For unvaccinated individuals we parameterise these using the central estimates from [9] for the duration of the proliferation and clearance phases and the peak Ct value. Profiles for vaccinated individuals use the same values for the duration of the two phases as for asymptomatic unvaccinated individuals (from [9]) but the peak Ct value is increased by 2 [11] for single (double) dose vaccinated individuals. The increased Ct value for a single dose is broadly in line with [15] [which found viral load to be 4-fold smaller after 1 dose of Pfizer vaccine, with mean Ct values in singly vaccinated individuals approximately 27 compared to 24.8 in unvaccinated. We could not find data on Ct values in doubly vaccinated individuals and assumed a further increase of 2 in the peak Ct value.

Results: In Fig. 6 we plot the contribution of each host type to the incoming viral load the be-
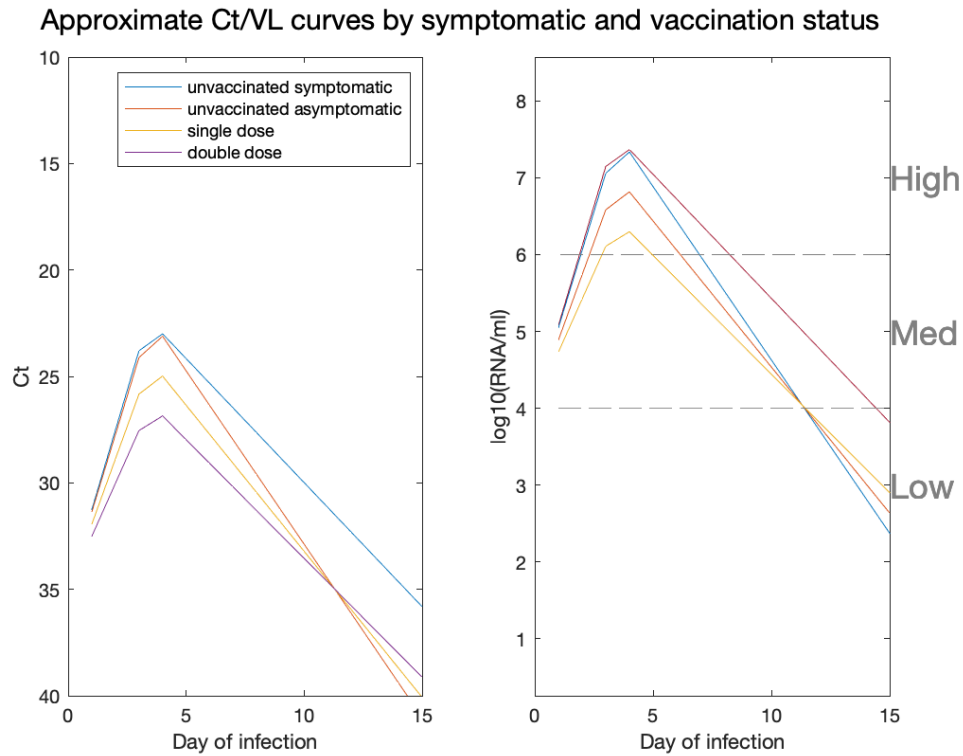
Figure 5: Assumed viral load profiles as measured by quantitative polymerase chain reaction (qPCR) Ct values (left) and ribonucleic acid (RNA) concentration (right), assuming conversion between the two from [9]. LFT sensitivity regimes are delineated by the dashed grey lines.

ginning of the event (panels a and b) and the total incoming viral load across all participants types (panel c), each in units Q. As anticipated from the input viral load trajectories, unvaccinated hosts provide the largest contribution and double-vaccinated hosts the smallest contribution.

Daily growth rates, with central estimates between -7% and +9%, have been reported approximately fortnightly for the UK epidemic since May 2020 [19]. Given the relatively slow clearance times in the adopted viral load curves, we may expect a higher viral load in a growing epidemic when there are more recently infected participants. We find that for perfect testing uptake, incoming viral load can almost double if the community growth rate is +10% compared to -10% per day. However, poor testing uptake has a relatively larger impact on incoming viral load for fixed prevalence: when the epidemic growth rate is zero the total incoming viral load is almost 9 times higher with no testing compared to perfect testing uptake in our simple model.

Extensions: This preliminary work is intended as a proof of principle and would need more
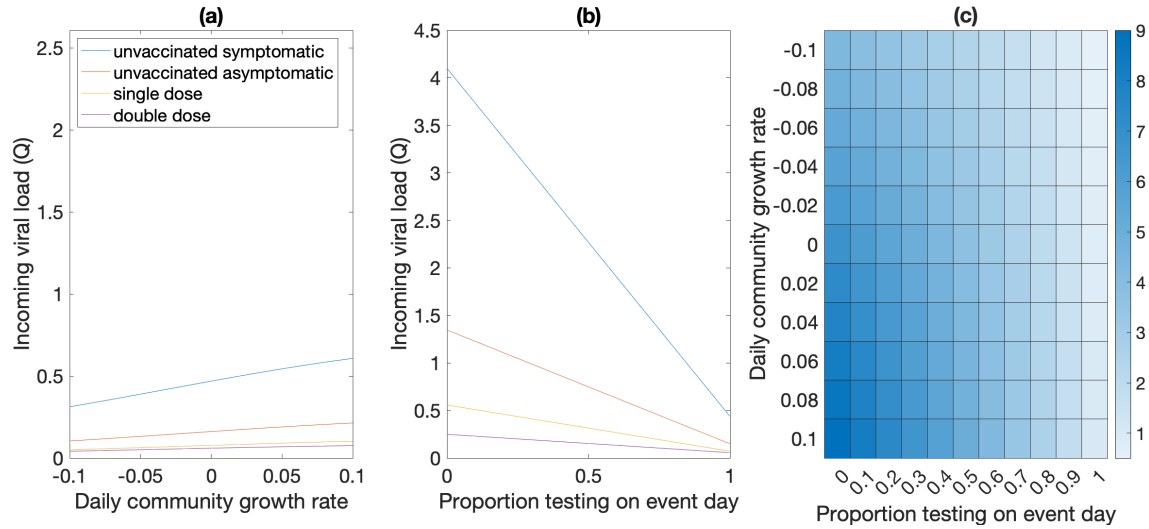
Figure 6: Incoming infectious quanta for event with N=10,000. In (a) we assume perfect testing uptake with lateral flow tests on the day of the event, and show the effect of community growth rate. In (b) we fix the growth rate to zero and explore testing uptake assuming uniform uptake across participant symptomatic and vaccination status. In (c) we plot total incoming viral load across participant types by testing uptake and growth rate. Quanta (Q) are measured in units of the maximum viral load of symptomatic participants.

work before it could be used in practice. There are many sensitivity analyses that warrant further attention, including:

- The age demographic of different events may vary widely, and future extensions of this model could consider this in conjunction with age-dependent vaccine uptake data (see Age Group Vaccination Status section below).

- Prevalence estimates can be rapidly evolving and now-casting may be useful to estimate the current prevalence in different participant types from recent infection data.

- Viral load dynamics are particularly uncertain for vaccinated hosts, and likely need to be re-evaluated for new variants. If the viral load is significantly higher for delta then this potentially aids detection with LFT but worsens the consequences of poor testing uptake. The shape of the viral load curve over the infection period in vaccinated hosts could be informed by considering the in-host viral dynamics (see section. 2.2.3 below).

- We have ignored delays from test result to entering the venue. This could be incorporated in an extension of the model.

- We have assumed that symptomatic participants only cancel their attendance if they test positive with a LFD, and the consequences of this assumption could be further explored.

2.2.2   Age Group Vaccination Status

The proportion of the population vaccinated with one or two doses varies considerably across age groups. We could use this information in an age-stratified extension of the venue viral load calculation above to explore how the viral load varies with the demographic profile of event attendees.

Table 3: Age banded vaccination proportion in England, estimated as at 13 July 2021 using data from [11] and [12].

	2020		2021 Proportion of Population	
Age groups	Estimated population	Vaccinated	Vaccinated 1st dose only	Vaccinated double dose
Under 25	16,802,877	0.1833	0.1292	0.0541
25 - 29	3,771,493	0.6596	0.4236	0.2360
30 - 34	3,824,652	0.7514	0.4442	0.3072
35 - 39	3,738,209	0.8027	0.4042	0.3985
40 - 44	3,476,303	0.8721	0.2385	0.6335
45 - 49	3,638,639	0.8780	0.1322	0.7458
50 - 54	3,875,351	0.9282	0.0457	0.8825
55 - 59	3,761,782	0.9533	0.0354	0.9179
60 - 64	3,196,813	0.9724	0.0267	0.9457
65 - 69	2,784,300	0.9582	0.0199	0.9383
70 - 74	2,814,128	0.9682	0.0167	0.9516
75 - 79	2,009,992	0.9970	0.0205	0.9765
80+	2,855,599	0.9696	0.0376	0.9320

Uncertainties

- We used the estimated population in 2020 to calculate these age banded vaccination proportions. The population estimates themselves are subject to uncertainty and the population will also have changed since 2020. Unreported vaccinations: in a day - 9.7%, within 7 days -2.9% [11]

- The vaccination data [11] gives the number of vaccinations administered in England, including individuals without an NHS number or no longer resident in England.

- The vaccination data [11] includes all individuals identified in the relevant age bands. In

particular the under 25 age group includes some children under 18 who have been vaccinated owing to risk factors or as a carer or health or social care worker.

2.2.3 In-host Viral Load Dynamics

The following set of ordinary differential equation (ODE) equations describe a TIVA model for modelling the in-host dynamics of viruses. The model described below is a simplified version of the TIVA model outlined in [16] that doesn't consider the eclipse phase of infected cells, nor does the model consider long term antibodies, memory cells or executor cells.

The model could be integrated to examine viral load dynamics over time with the ultimate aim of providing more detailed information on how this is affected by vaccination.

TIVA Model

$$\frac{dT}{dt} = -\beta VT \tag{1}$$

The number of transfer cells (T) that are infected by virus particles (V) increases at a rate β. Possible to include an *eclipse* phase where infected cells don't shed virus particles for some amount of time.

$$\frac{dI}{dt} = \beta VT - \delta I - \epsilon AI \tag{2}$$

The number of cells (I) infected by virus particles (V) increases at a rate β and decreases (through cell death) at a rate δ. Antibodies (A) remove infected cells at a rate ϵ.

$$\frac{dV}{dt} = \rho I - \phi V - \sigma AV \tag{3}$$

The number of virus particles (V) created by infected cells (I) increases at a rate of ρ and decreases (through shedding) at a rate ϕ. Antibodies (A) remove virus particles at a rate σ.

$$\frac{dA}{dt} = \kappa V \tag{4}$$

The number of antibodies (A) created in response to virus cells (V) increases at a rate κ. Some example solution trajectories are shown below.

Extensions

- Integrate model with trustworthy initial condition and rate parameters (such as those estimates by previous studies, e.g. [17])

- The current model assumes that cells generate new viral particles as soon as they become infected, which is not realistic. An *eclipse phase* can be introduced to account for this behaviour as in [16].

- Model the evolution of long term antibodies and memory cells and their effect on future viral infection.

- Separate the responsibility of removing viral particles and infected cells between antibodies and executor cells respectively.

- Define model in a probabilistic programming language (PPL) such as Stan [18] and fit to real data, such as that presented in Ref. [9].

2.3   Can ventilation be designed to minimise the virus concentration in a room?

Aim: We consider the problem of ventilating indoor spaces when people infected with COVID19 may be present. We present the beginning of a theoretical framework which could be optimised to advise on the best placement of ventilation units to minimise the COVID19 concentration in an events space.

2.3.1   Governing equations for the ventilation problem

Let $\mathbf{x} = (x, y, z)$ denote the spatial variable associated with the principle $x-$, $y-$ and $z-$ directions. We consider a sufficiently large room Ω defined according to

$$\Omega := \{(x, y, z) : 0 < x < L, 0 < y < W, 0 < z < H\},$$

and having volume $V = WLH$.

We assume for simplicity that there is one person in the room breathing constantly or talking. This person is infected with COVID19 and emits the virus at a rate R. We treat the person as

a source in the mathematical problem. Note the model described below can be generalised to the case when there are multiple people in the room and a distribution characterising their positions is known.

Additionally, separated from the lateral walls and the ceiling of the the room are ventilators that extract air from the room as well as supplying fresh air. Due to the size of the ventilators in comparison with the room, we will model their effect as point sinks.

The concentration of the virus c within the room is treated as a function of $\mathbf{x}$ and t. It satisfies the partial differential equation:

$$
\begin{aligned}
\frac{\partial c}{\partial t} &+ \boldsymbol{\nabla} \cdot (\mathbf{u}c) \\
&= \frac{R}{V}\delta(\mathbf{x} - \mathbf{x}_p) - \sum_{j=1}^{N} \lambda_j c(\mathbf{x}_j)\delta(\mathbf{x} - \mathbf{x}_j) \qquad \text{for } \mathbf{x} \in \Omega, t > 0 .
\end{aligned}
\tag{5}
$$

Here, λ_j, $1 \leq j \leq N$, are the air exchange rates owing to the ventilators we assume are known. Further, $\mathbf{u}$ is a velocity profile for the air contained in the room, having density ρ and subjected to gravity. The pressure inside the room is $p(\mathbf{x})$.

We assume the flow inside the room corresponds to a small Reynolds number regime. Additionally, we assume the typical airflow attributed to an air conditioning unit is small in comparison to the speed of sound [**?**], allowing us to model the air as an incompressible fluid. Thus, $\mathbf{u}$ satisfies the Stokes problem:

$$
\begin{aligned}
-\rho g\mathbf{e}_z + \mu\nabla^2\mathbf{u} = \boldsymbol{\nabla}p + \sum_{j=1}^{N} \mathbf{V}_j\delta(\mathbf{x} - \mathbf{x}_j) \qquad &\text{for } \mathbf{x} \in \Omega, \\
\boldsymbol{\nabla} \cdot \mathbf{u} = 0 \qquad &\text{for } \mathbf{x} \in \Omega ,
\end{aligned}
\tag{6}
$$

where $\mathbf{V}_j$, $1 \leq j \leq N$, represent the forcing orientation and intensity connected with the jth ventilator, which we assume can be specified. Finally, we close the system corresponding to this approximate model by supplying boundary conditions on the velocity $\mathbf{u}$ and c, and where relevant, initial conditions.

We assume the air cannot penetrate the walls and thus we set

$$\mathbf{u} = \mathbf{0} , \qquad \mathbf{x} \in \partial\Omega ,$$

$$\frac{\partial c}{\partial \mathbf{n}} = 0 , \qquad \mathbf{x} \in \partial\Omega , t > 0 ,$$

where $\mathbf{n}$ is the unit outward normal to the room walls. Finally, we assume their is no concentration of the virus initially, i.e.:

$$c(\mathbf{x}, 0) = 0 , \qquad \mathbf{x} \in \Omega .$$

2.3.2 Solution to the Stoke's problem

To facilitate the solution to the viral load problem, we now present the solution to the Stoke's problem which can then be readily inserted into (6). This field utilises the solutions to model problems which are described below. The velocity field $\mathbf{u}$ admits the form:

$$\mathbf{u}(\mathbf{x}) = \mathbf{u}_0(\mathbf{x}) + \sum_{j=1}^{N} \mathbf{G}(\mathbf{x}, \mathbf{x}_j)\mathbf{V}_j . \tag{7}$$

Here, $\mathbf{u}_0$ is the solution (6) in the absence of the point sources, i.e. no ventilators. The matrices $\mathbf{G}$ represents Green's tensor for the domain Ω.

Green's tensor in Ω: We introduce the Green's tensor $\mathbf{G}$ for the Stokes's problem:

$$\mu \nabla^2 \mathbf{G}(\mathbf{x}, \mathbf{y}) = (\boldsymbol{\nabla} \otimes \mathbf{p}(\mathbf{x}, \mathbf{y}))^{\mathrm{T}} + \delta(\mathbf{x} - \mathbf{y})\mathbb{I}_3 \qquad \text{for } \mathbf{x} \in \Omega,$$

$$\nabla \cdot \mathbf{G}(\mathbf{x}, \mathbf{y}) = \mathbf{0}^{\mathrm{T}}$$

where $\mathbf{p} = (p_1, p_2, p_3)^{\mathrm{T}}$, having entires p_1, p_2 and p_3 representing the pressure fields for the first, second and third columns of $\mathbf{G}$. This tensor also satisfies the homogeneous boundary conditions

$$\mathbf{G}(\mathbf{x}, \mathbf{y}) = 0\mathbb{I}_3 , \qquad \mathbf{x} \in \partial\Omega .$$

Further, $\mathbf{G}$ may be written as

$$\mathbf{G}(\mathbf{x}, \mathbf{y}) = \mathbf{J}(\mathbf{x} - \mathbf{y}) - \mathbf{H}(\mathbf{x}, \mathbf{y})$$

where $\mathbf{H}$ is the regular part of $\mathbf{G}$ and $\mathbf{J}$ is the Oseen tensor satisfying:

$$\mu \nabla^2 \mathbf{J}(\mathbf{x}) = (\boldsymbol{\nabla} \otimes \mathbf{p_J}(\mathbf{x}))^{\mathrm{T}} + \delta(\mathbf{x})\mathbb{I}_3 \qquad \text{for } \mathbf{x} \in \mathbb{R}^3.$$

Here, the Oseen tensor has the form:

$$\mathbf{J}(\mathbf{x}) = \frac{1}{8\pi\mu|\mathbf{x}|}\left(\mathbb{I}_3 + \frac{\mathbf{x}\mathbf{x}}{|\mathbf{x}|^2}\right)$$

with $\mathbf{p_J}$ being

$$\mathbf{p_J}(\mathbf{x}) = \frac{\mathbf{x}}{4\pi|\mathbf{x}|^3} \ .$$

The function $\mathbf{u}_0$: Additionally, require the solution to the problem involving a gravitational load:

$$-\rho g\mathbf{e}_z + \mu\nabla^2\mathbf{u}_0 = \boldsymbol{\nabla}p_0 \qquad \text{for } \mathbf{x} \in \Omega,$$

$$\nabla \cdot \mathbf{u}_0 = 0 \qquad \text{for } \mathbf{x} \in \Omega,$$

$$\mathbf{u}_0 = 0 \ , \qquad \text{for } \mathbf{x} \in \partial\Omega \ .$$

In fact, the solution to this problem for any Ω takes the form:

$$\mathbf{u}_0 = 0 \ , \qquad p_0 = -\rho gz \ . \tag{8}$$

Substitution of into allows us to update the velocity field to

$$\mathbf{u}(\mathbf{x}) = \sum_{j=1}^{N}\mathbf{G}(\mathbf{x}, \mathbf{x}_j)\mathbf{V}_j \ . \tag{9}$$

where it remains to construct $\mathbf{G}$.

2.3.3 Further work

- it is intended to use the representation of $\mathbf{u}$ in (9) to lighten the required computational load via numerical approaches to investigating the concentration c according to (6).

- it seems possible to compute $\mathbf{G}$ for relatively simple geometries Ω, which will be a next step for advancing this problem for the room represented by a rectangular prism.

- the eventual aim of the above model would be to attempt to engage optimisation problems whereby the ventilator properties and their positions can be optimised to minimise the virus concentration over the entire room in time t for a group of people distributed across the room.

2.4 Conclusions & Future work

Can we control the length and geometry of a queue to minimise infection risk?

- The risks of queuing to those in a queue and serving queues are considered. The contributions to the cumulative 'viral dose' are generally much lower from infected ticketers (those serving queues) apposed to infected attendees nearby in the queue. This is because queuers spend relatively little time with the ticketer. However, as each ticketer meets many people, this risk can rise to significant levels if the prevalence is high.

- Introducing multiple entry time slots may reduce the risk of infection of event attendees while queuing by reducing the number of individuals in the queue. In our simulations four time slots seem to significantly reduce risk. However, this may be parameter dependant.

- The model suggests that fewer long rows reduce the number of individuals at risk o infection. However, this is likely to be dependant on the choice of cumulative 'viral dose' which determines whether an individual is at risk.

- In the models we conclude that an individual is 'at risk' if there cumulative risk is above a set value. However, the probability of infection is likely to increase with viral dose, with some people becoming infected with low levels of exposure to the virus.

- Our assumption that a critical viral load must be reached for an individual to become at risk of infection may underestimate the ability of an infected ticketer to transmit the virus to attendees. For an interaction to be dangerous the serving time would need to last almost a minute. The distribution of ticketing times means this is extremely rare within our model.

- We set the probability of an individual attending the event to 2%, however this is likely to be dependent on the demographic of the event and testing regimes prior to the event. Work from the testing group could therefore probably improve the accuracy of this estimate.

- In future work, we would need to account for the fact some individuals pay no attention to time slots.

- This work could easily be adapted to model an unticketed event. Here the distribution of expected arrival times and time taken to process a ticket could be adapted to explain a different event type.

- Individuals may be more likely to arrive at an event in groups opposed to individuals. The size of the groups arriving could be assigned by the distribution of the number of tickets bought together.

- Finally, many events will be recurring. We can improve our model for future events using data from prior events through the use of statistical inference.

Can we estimate the viral load at a venue given a certain testing regime?

- Unvaccinated hosts provide the largest contribution to incoming viral load and double-vaccinated hosts the smallest contribution.

- We may expect a higher viral load in a growing epidemic when there are more recently infected participants. In our simple model we find that for perfect testing uptake, incoming viral load can almost double if the community growth rate is +10% compared to -10% per day. However, poor testing uptake has a relatively larger impact on incoming viral load for fixed prevalence.

- The age demographic of different events may vary widely, and future extensions of this model could consider this in conjunction with age-dependent vaccine uptake data.

- Prevalence estimates can be rapidly evolving and now-casting may be useful to estimate the current prevalence in different participant types from recent infection data.

- Viral load dynamics are particularly uncertain for vaccinated hosts, and likely need to be re-evaluated for new variants. If the viral load is significantly higher for delta then this potentially aids detection with LFT but worsens the consequences of poor testing uptake. The shape of the viral load curve over the infection period in vaccinated hosts could be informed by considering the in-host viral dynamics.

- We have ignored delays from test result to entering the venue. This could be incorporated in an extension of the model.

- We have assumed that symptomatic participants only cancel their attendance if they test positive with a LFD, and the consequences of this assumption could be further explored.

- The model presented on in-host viral dynamics needs further refinement including: introduction of an eclipse phase between cell infection and generation of new viral particles; modelling the evolution of long term antibodies and memory cells and their effect on future viral infection; separation of the responsibility of removing viral particles and infected cells between antibodies and executor cells respectively; fitting to real data.

- The venue viral load calculator could be developed further including some or all of these additional features to inform on the relationship between age-stratified SARS-CoV-2 infection prevalence, event demographics, in-host viral dynamics, test and trace strategies, and their impact on possible total venue viral load at large events.

Can ventilation be designed to minimise the virus concentration in a room?

- The eventual aim of the ventilation model proposed in this report would be to attempt to create optimisation problems whereby the ventilator properties and their positions can be optimised to minimise the virus concentration over the entire room in time t for a group of people distributed across the room. Further work is needed to validate the model, and implement it.

References

[1] Z. Lau, I.M. Griffiths, A. English, K. Kaouri (2021): Predicting the Spatially Varying Infection Risk in Indoor Spaces Using an Efficient Airborne Transmission Model, `https://arxiv.org/pdf/2012.12267`

[2] Q. Cao, et al. (2021): An experimentally validated analytical model for aerosol number conctration reduction in classrooms, Aerosol and Air Quality Research 21, no. 9, 210038. `https://doi.org/10.4209/aaqr.210038`

[3] S. Millar et al. (2020): Transmission of SARS-CoV-2 by inhalation of respiratory aerosol in the Skagit Valley Chorale superspreading event, Indoor Air 31:314–323. `https://onlinelibrary.wiley.com/doi/epdf/10.1111/ina.12751`

[4] Pierrot Derjany, Sirish Namilae, Dahai Liu, and Ashok Srinivasan, Multiscale model for the optimal design of pedestrian queues to mitigate infectious disease spread `https://journals.plos.org/plosone/article?id=10.1371/journal.pone.0235891`

[5] G. Buonanno, L. Stabile, and L. Morawskab, Estimation of airborne viral emission: Quanta emission rate of SARS-CoV-2 for infection risk assessment `https://www.ncbi.nlm.nih.gov/pmc/articles/PMC7211635/`

[6] C. Budd, K. Calvert, S. Johnson, and S. O. Tickle, Assessing risk in the retail environment during the COVID-19 pandemic `https://royalsocietypublishing.org/doi/10.1098/rsos.210344`

[7] Delong Li, An Airport Diversion Security Inspection Model Based on Epidemic Prevention and Control in the Period of COVID-19 `https://www.dpi-proceedings.com/index.php/dtetr/article/view/35010/33592`

[8] Airborne transmission calculator: `https://docs.google.com/spreadsheets/d/16K1OQkLD4BjgBdO8ePj6ytf-RpPMlJ6aXFg3PrIQBbQ/edit#gid=519189277`

[9] Kissler et al (2021) `https://journals.plos.org/plosbiology/article?id=10.1371/journal.pbio.3001333`

[10] REACT round 13: `https://spiral.imperial.ac.uk/bitstream/10044/1/90197/2/react1_r13_interim_preprint.pdf`

[11] NHS England Vaccinations (13/07/2021) (`https://www.england.nhs.uk/statistics/wp-content/uploads/sites/2/2021/07/COVID-19-daily-announced-vaccinations-13-July-2021.xlsx`

[12] Office of National Statistics (2020) `https://www.ons.gov.uk/peoplepopulationandcommunity/populationandmigration/populationestimates/bulletins/annualmidyearpopulationestimates/mid2020#age-structure-of-the-uk-population`

[13] Oran, D. P., & Topol, E. J. (2021). The Proportion of SARS-CoV-2 Infections That Are Asymptomatic : A Systematic Review. Annals of internal medicine, 174(5), 655–662. `https://doi.org/10.7326/M20-6976`

[14] DHSC LFT performance evidence published 07 July 2021: `https://assets.publishing.service.gov.uk/government/uploads/system/uploads/attachment_data/file/999866/asymptomatic-testing-for-SARS-CoV-2-using-antigen-detecting-lateral-flow-devices-evidence-from-performance-data-Oct-2020-to-May-2021.pdf`

[15] Matan Levine-Tiefenbrun, Idan Yelin, Rachel Katz, Esma Herzel, Ziv Golan, Licita Schreiber, Tamar Wolf, Varda Nadler, Amir Ben-Tov, Jacob Kuint, Sivan Gazit, Tal Patalon, Gabriel Chodick, Roy Kishony. Decreased SARS-CoV-2 viral load following vaccination. medRxiv 2021.02.06.21251283; doi: `https://doi.org/10.1101/2021.02.06.21251283`

[16] Ruian Ke *et al*, Daily sampling of early SARS-CoV-2 infection reveals substantial heterogeneity in infectiousness. doi: `https://doi.org/10.1101/2021.07.12.21260208`

[17] Cao, Y, Gao, W, Caro, L, Stone, JA. Immune-viral dynamics modeling for SARS-CoV-2 drug development. Clin Transl Sci. 2021; 00: 1–12. `https://doi.org/10.1111/cts.13099`

[18] Stan Development Team. 2021. Stan Modeling Language Users Guide and Reference Manual, 2.27. `https://mc-stan.org`

[19] The R value and growth rate `https://www.gov.uk/guidance/the-r-value-and-growth-rate#history`

3 Outside & ticketed

This section considers how to limit the risk of COVID19 transmission in events which are outside and ticketed. This section considers in particular the specific use case of Bath Rugby Stadium, shown in Fig. 7.

Figure 7: Bath Rugby Stadium

During the discussion, the group considered two parts of the inside-stadium event which are most risky; arrival and half-time. **The arrival** - because many events are taking place in towns, people are arriving late (70 % arrive in the last 20 - 30 minutes) which creates large queues and therefore an increase risk of infection. The other challenge is in stadium - mostly **at half time** with people going to the toilet, walking past each other to bars etc, this again creates a higher risk situation. Another scenario was considered where people leave the stadium at the end of a match. Speaking with event management professionals, however, it was felt that the half-time issue was most risky. For both situations we are trying to understand how we can model the spread of COVID19 and how our actions can limit this risk.

For the **arrival** scenario, the group considered three aspects; the modelling and reduction of of queue length, impact of COVID19 checking, and seat allocation depending on COVID19 status.

For the **half-time** scenario, the group considered the flow (and contacts) of people during half-

time heading to bars, and how to model the impact of good signage.

3.1 Can we model and mitigate risk from an events arrival process?

Given the potential for a large number of contacts to occur at the arrival stage of a large event, the below considers some approaches which model the impact of pre-checking and fast-tracking on queue lengths.

3.1.1 Reduction and modelling of queue length

We consider how people might be infected with COVID19 in a long queue, can some of the ideas below be used to manage an effective queue system whereby people do not need to be in the queue for the whole time?

- **Allocate arrival slots** and gates on ticket booking with possibility of re-booking

- **Pre-screening off site** hours before a match, fast-track lanes for pre-checked

- Show **live queuing numbers online**, register for entering

- **Incentives to arrive early**, e.g. seat service, which allows to view players warm up

Arrival rate: given the conversations with the security officer at the VSG, the group considered a scenario whereby 70% of the attendees arrive in the last 30 minutes, as such we use the beta distribution, whose density is shown in Fig. 8 (left) to approximate this arrival rate. In Fig. 8 (right) we approximate the arrival rate if we allow pre-checking using a fat-beta distribution.

Using the fat-beta distribution for the pre-arrival rate, the group considered the impact this would have on the length of queue and time taken to admit several hundred into the stadium. In Fig. 9 (left) the performance of one queue is assessed, which takes over 350 minutes to admit everyone (assuming a 30 second check per attendee). However, if we use two queues as shown in Fig. 9 (right) we can reduce the time to check all tickets to around 150 mins, If we want to get every single audience assuming several hundred for each stands get all the checking done. within this time, it is not working well - takes over 350 minutes. But if we have two qs we can check tickets that can reduce to 150 mins.
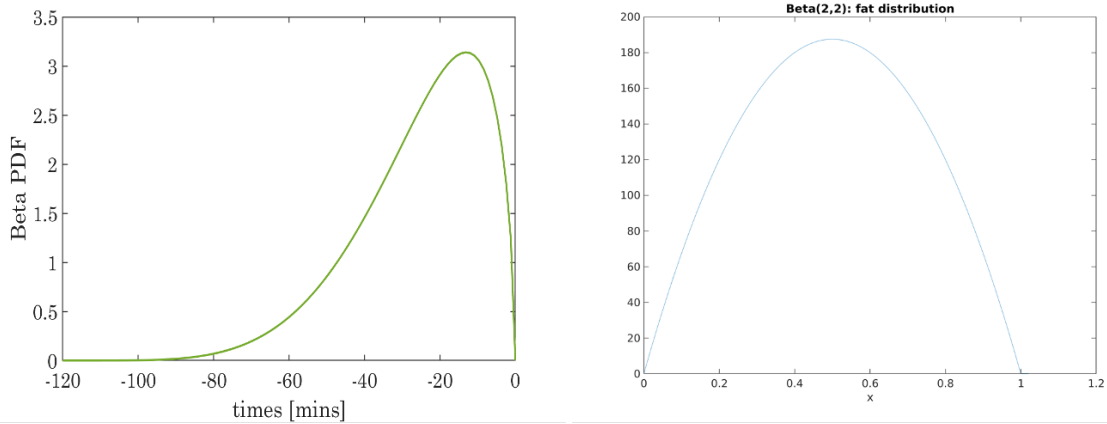
Figure 8: (left) 70 % audience arrives before match starts (right) audience arrives for pre-checking
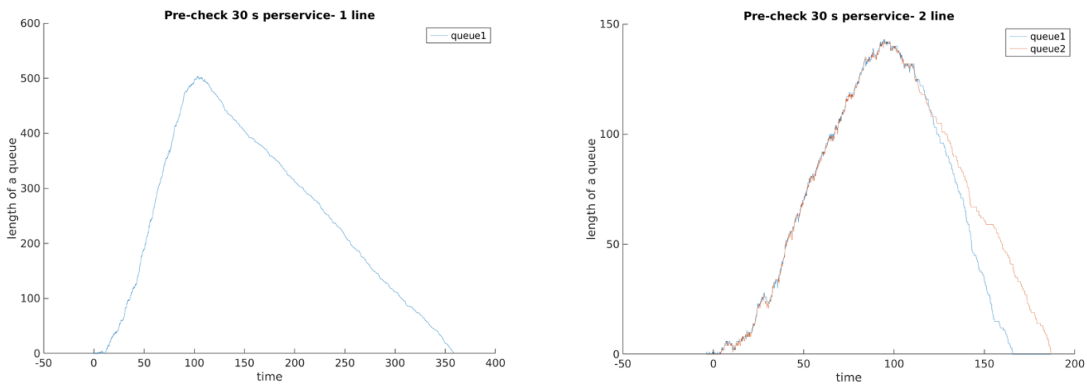

Figure 9: (left) Pre-check 30 second pre-service, 1 line (right) Pre-check 30 second pre-service, 2 line.

In a case where we do not consider COVID19; there are no temperature checks, LFT checks, etc, then we can possibly do the remaining checks in 12 seconds per person. In this normal case Fig. 10 (left) shows that with three queues, the length of each queue is around 9 people, again assuming the beta arrival distribution in Fig. 8 (left). However, when the longer checks are required, and the arrival profile assumes 70% in the 30 minutes building up to a game, the queue lengths are shown in Fig. 10 (right); around 120 people in each queue, and queuing extending 50 minutes into the match!

How can we balance a scenario where slow checking (30 second) and pre-checking can be used together? In Fig. 11 (left) we see the impact of the queue from slow-checking with no pre-checking done - close to 120 people in a queue. However, if we can manage it so that 40% of the attendees are pre-checked, then we can reduce the queue length to 35. The queue length decreases even more if 60% of the audience is pre-checked etc.
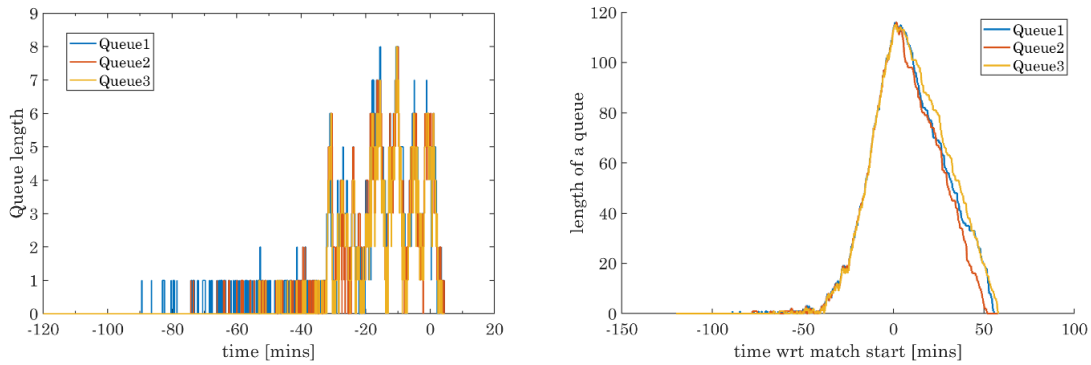
Figure 10: (left) Current check-in time (12 second for check in) (right) Check-in involving temperature check (30 seconds for check in)
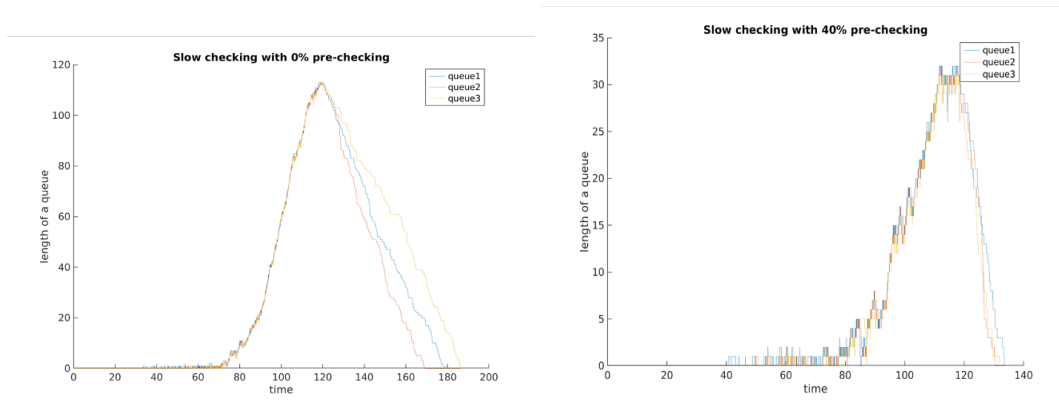

Figure 11: Slow checking (30 seconds per customer) with (left) and without (right) pre-checking

Another question we might reasonably ask is if we can manage to pre-check everyone, and they all rush back, what will happen to the queue lengths? This assumes 100% of the audience is pre-checked and walk in an a **green pass**. Fig. 12 (left) shows the situation if 70% the green pass attendees all arrive back within the 15 minutes building up to a game, causing queues of up to 60 people. However, if they can be encouraged to stagger their arrival back over the 30 minutes building up to a game, the highest number of people in a queue is around 10 people, waiting less than half a minute in the queue.

Fig. 13 (left) shows the number of people waiting in a queue [FOR WHICH SCENARIO?] and for how long they are waiting. People who get before the queue formed can get in in approximately 30 seconds (mean check in time). Fig. 13 (right) shows how the time spent waiting in a queue depends on the time at which the queue is join, the waiting time increases significantly the closer to the event you get.

Finally, Fig. 14 shows the average waiting time per person in a queue based on the number of
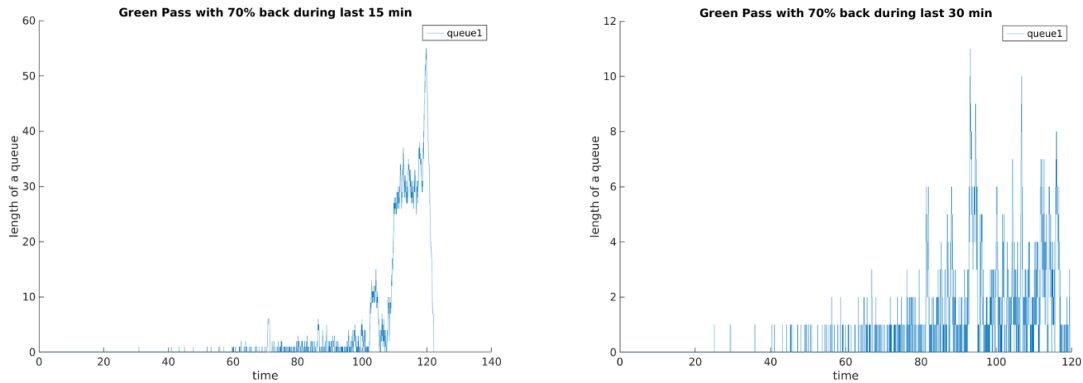
**Figure 12:** 70 % people enter the Green pass within the last (left) 15 minutes and (right) 30 minutes.
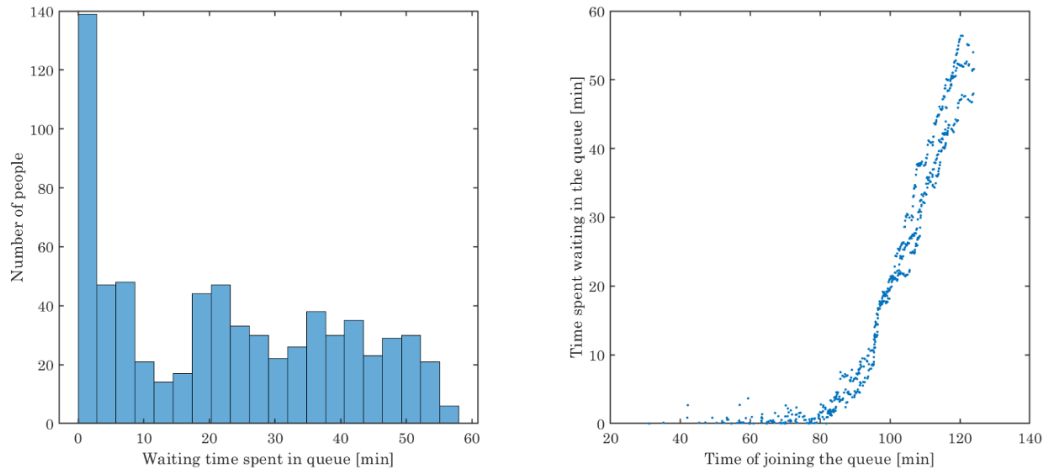
Figure 13: (left) the number of people and the time they spend in a queue (right) impact of arrival time on time spent in a queue.

people who have been pre-checked. In the case where 700 people are being admitted, anything above 400 (even with slow check-in time) results in an average waiting time of around 30 seconds.

### 3.1.2 Seat allocation to reduce infection risk

This section considers how information around peoples vaccination status could be used in the allocation of seats. This obviously assumes that attendees are willing to volunteer their status when buying a seat. Could this information then be used to advise where in the stadium there is a likely lower risk? Fig. 15 shows diagrammatically how stadium attendees could be
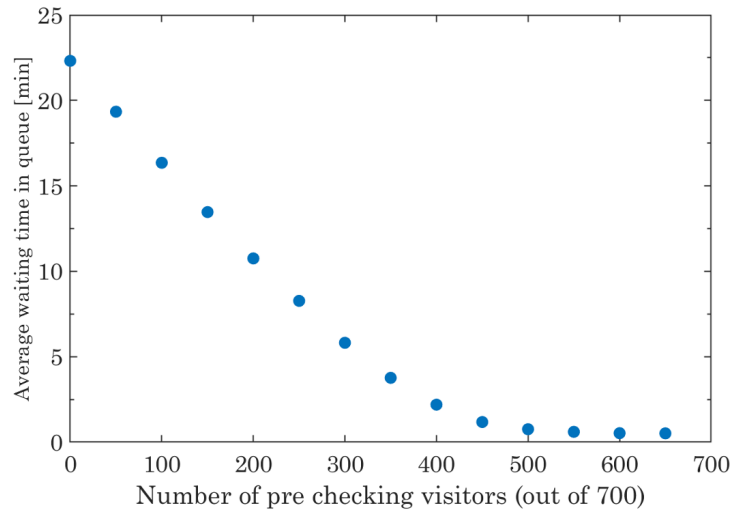
Figure 14: Average waiting time in queue as a function of pre-checked proportion. Each dot is based on the mean from 100 Monte Carlo simulations.

depicted.
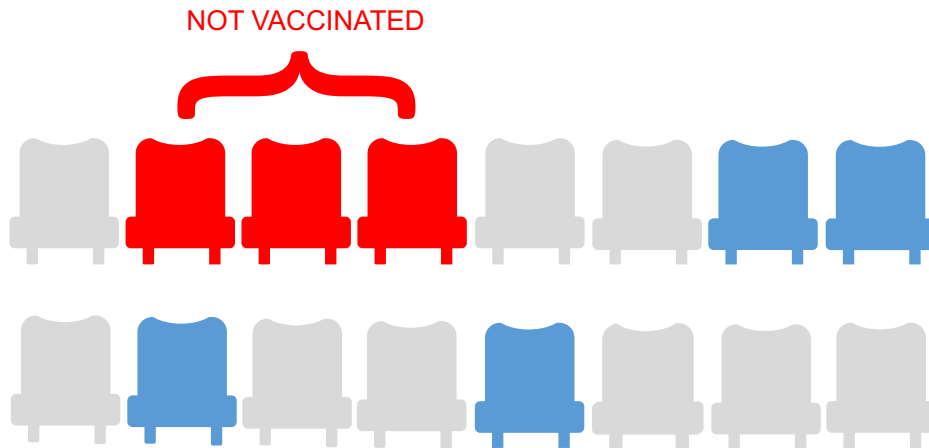
Figure 15: Unvaccinated and vaccinated attendees at a stadium.

Eq. (10) describes a very simple mathematical model which describes the viral dose which would be obtained by sitting at a given position. The model uses an inverse square law which assumes that the amount of infection received decreases as $1/r^2$, where r is the distance between someone and an infected person.

$$DOSE(\mathbf{x}) = p_{UI} = \sum_{i \in US} \frac{1}{(\mathbf{x} - \mathbf{x}_i)^2} + p_{VI} \sum_{i \in VS} \frac{1}{(\mathbf{x} - \mathbf{x}_i)^2} \tag{10}$$

where:

- p_{UI} is the probability that an unvaccinated person is infected

- US are the seats occupied by unvaccinated people (red in fig. 15)

- p_{VI} is the probability that a vaccinated person is infected

- VS are the sears occupied by vaccinated people (blue in Fig. 15)

Preferential allocation? Is there a preferential allocation of seating so as to advise attendees which ones should be avoided if you are unvaccinated? For example, in Fig. 16, can we disable some seats given some expected high viral load?
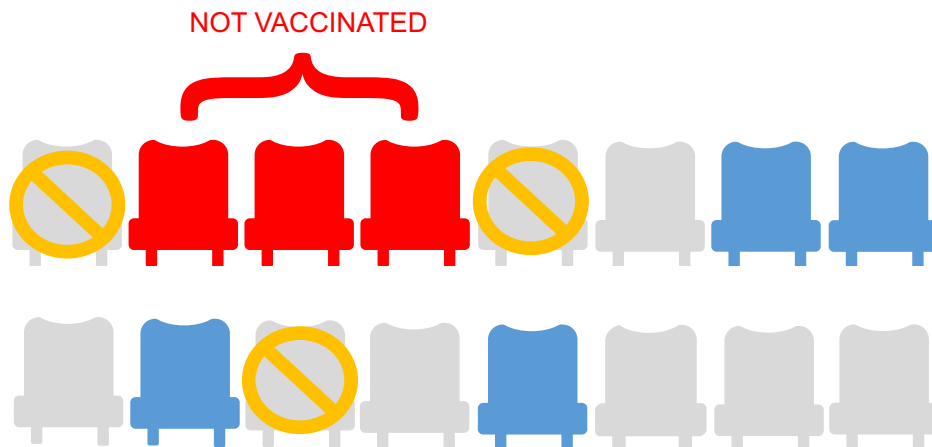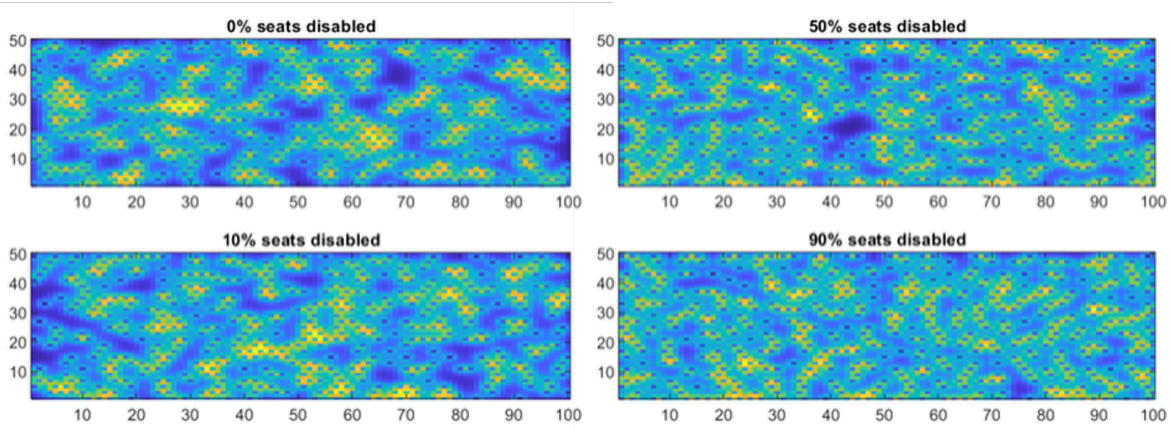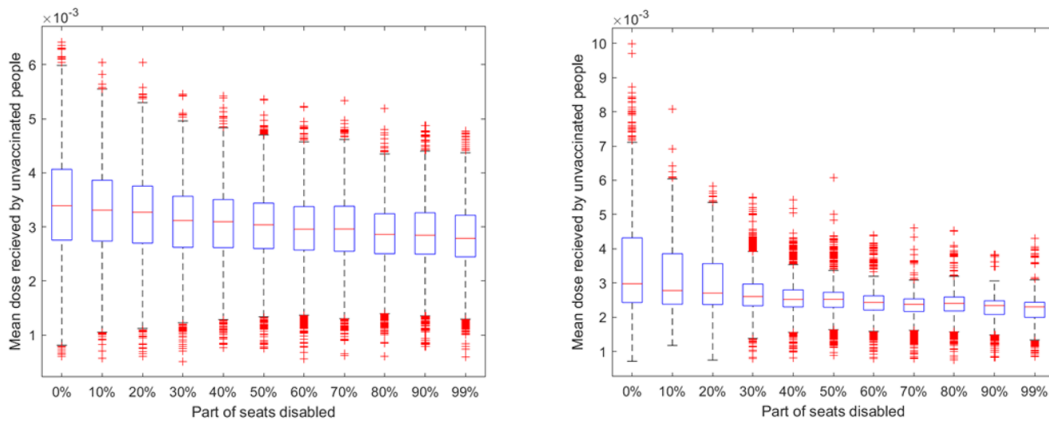

Figure 16

Fig. 17 shows the risk heatmap for where 0, 10, 50 and 90 % of the seats are disabled for the unvaccinated people to sit in. Can we suggest that the unvaccinated / potetnially infectious people to spread across the stadium so that we don't see the heatspots you can see in the completely random scenario.

However, what is seen in Fig. 18 is that if we increase the number of seats which are disabled significantly, the mean dose received is not increased significantly. A tentative recommendation is that no matter how many groups are vaccinated, allocating based on vaccination status is not the intervention to be pursued.

Figure 17: Transmission risk heatmap with 9, 10, 50 and 90 % of the seats disabled.


Figure 18: Mean dose received by unvaccinated people over entire match for (left) 60 % people vaccinated (right) 90 % people vaccinated.

3.2   Can we model and mitigate the risk of crowds using events facilities?

This section considers the issue and potential transmission risk of what happens after people are seated, in particular people going to the bar / toilet at half-time, and when they leave the stadium. The group discussed the impact of compliance by attendees, whether the home team wins or loses, number of attendees, proportion vaccinated, the weather. After discussion with a security expert, it was decided that the focus should be on halftime movement.

3.2.1   Control of people during half-time

The group considered a model which assumes the paths taken at half-time to a number of bars around the stadium is that shown in Fig. 19
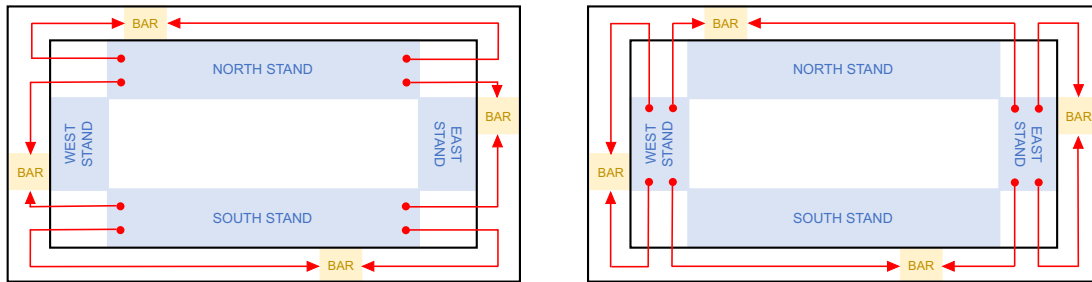

Figure 19: Routes taken by attendees to bars from (left) north and south and (right) east and west stands. Note, in the simulation there is symmetry between the opposite sides.

Simulated audience position: Fig.22 show the time evolution of the simulation. Top-left shows the initial seated condition. The simulation then tracks attendees over half-time and measures the interaction. The model assumes that attendees act rationally and leave their stand on the nearest side and then go to the nearest bar. It assumes that the attendees return their seats using the same path. The time profile by which attendees leave their seats to go to the bar is approximated by a Gamma distribution. The stadium is assumed to be at 40% attendance. It is also assumed that people stay at the bar for a uniformly random amount of time (a proper queue model could be added in the future.)

The group considered different gamma distributions to approximate the time profile by which attendees leave their seats. Fig. 21 (left) shows the total number of contacts made over the simulation for three time profiles; $\sigma = 15$, $\sigma = 2$ and a uniform random distribution over 50 minutes (when half-time ends). With $\sigma = 2$ people leave their seats as quickly as they can and therefore have a lot of contacts at the beginning resulting in the most total number of contacts during half-time. For the $\sigma = 15$ case, people wait a little longer before leaving, reducing the number of contacts. The uniform case over the half-time break results in the least number of contacts. This provides some evidence to suggest that staggering the times at which people go to the bar has an effect on reducing the potential infection risk.

Finally, we consider lifting the assumption of rational behaviour of the attendees which caused attendees to go to specific bar which avoided the most number of people. We introduce a probability parameter p of people making the wrong choice in their route - an element of **confusion**. The purpose of this is to investigate the impact of effective signage on contact numbers.
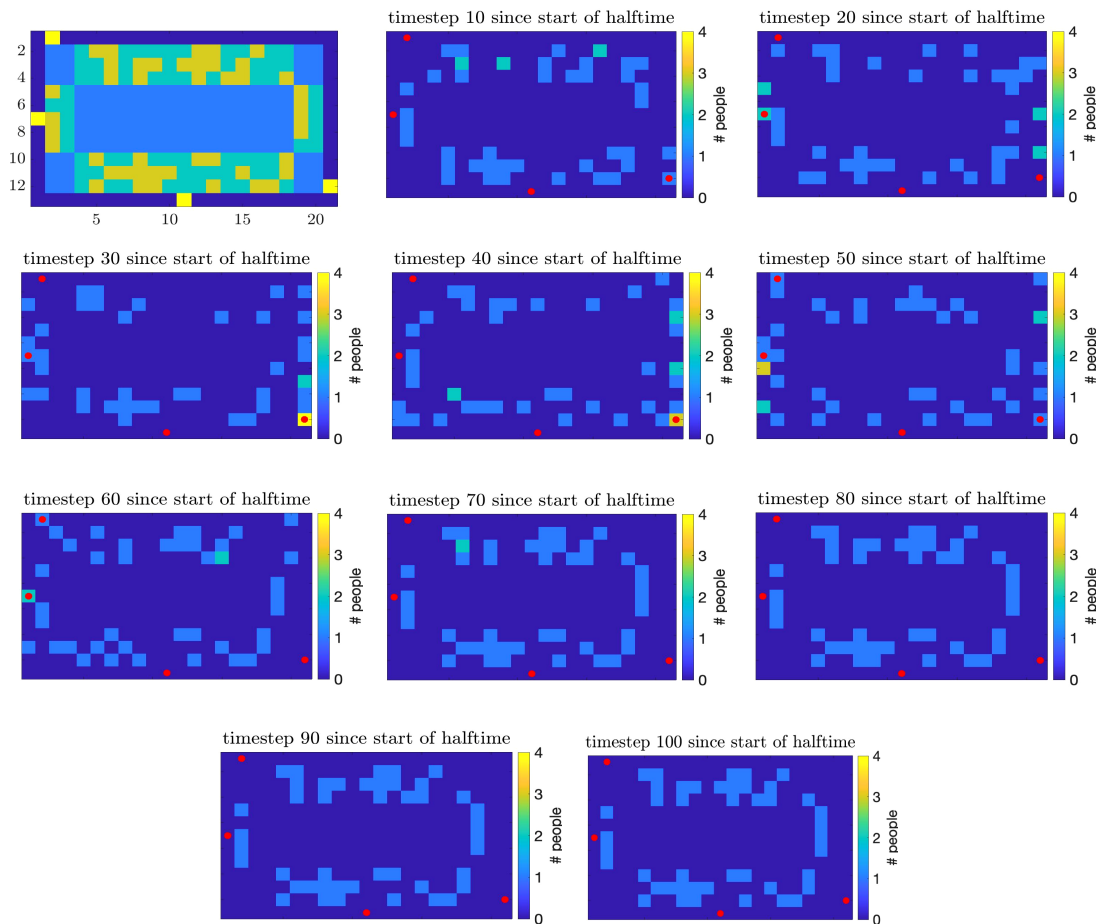
Figure 20: Half-time simulation. (Top left) initial position of attendees. initial position of attendees, location of bars, stands, and corners without seats.

In Fig. 21 (right) we show the different values of p, 0 means no confusion (i.e. everyone goes to the bar they are expected to go to). However, if p goes up to 50 %, the number of contacts go up. An interesting extension would be to consider what happens the the contacts as a function of confusion (p, and the number total number of attendees in the stadium.

3.2.2 Future work

- Include people going to the toilet as well

- Include a more realistic queuing model

- How the impact of confusion scales with the number of attendees

- Compare people going to the bar versus servers bringing drinks to seats
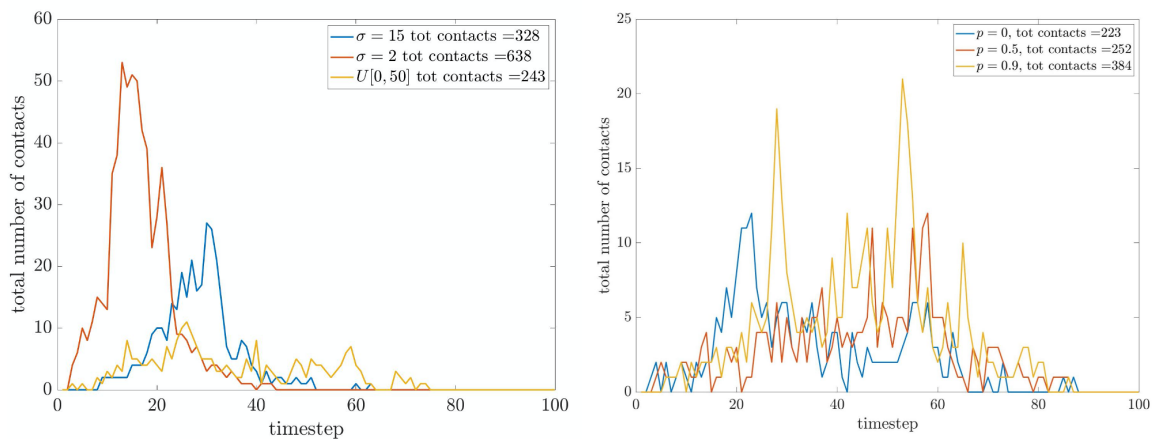
Figure 21: (left) Simulation of total number of contacts made over half-time whilst visiting a bar for three time profiles explained in the text. (Right) Number of contacts over half-time as a function of attendee confusion.

3.3 Conclusions & future work

Can we model and mitigate risk from an events arrival process?

- Pre-checking is useful to reduce waiting time in case if longer temperature measurement, LFT checks etc are necessary. A combination of pre-checking and late arrivals for these long checks has been modelled to look at the impact on queue length and time spent in the queue.

- Early modelling suggests that preferential allocation of seats based on vaccination status does not seem to reduce infection risk significantly. It was suggested by the group that the best way to reduce it, is to minimise the chance of allowing infected people to the stadium.

Can we model and mitigate the risk of crowds using events facilities?

- An agent-based model was used to simulate the movement of people during half-time to nearby bars, and monitor the number of contacts made during this movement. The group modelled the impact of different time profiles by which people leave their seats. This modelling suggests that people should be encouraged to stagger their half-time bar trips to reduce the number of contacts made.

- The model allows for some level of confusion, by which people do not go to their 'nearest'

bar. This confusion increases the number of likely contacts. Therefore, effective sign-posting can be a useful method in reducing potetnial transmission.

References

[1] Multiscale model for the optimal design of pedestrian queues to mitigate infectious disease spread. Derjany P, Namilae S, Liu D, Srinivasan A (2020) Multiscale model for the optimal design of pedestrian queues to mitigate infectious disease spread. PLOS ONE 15(7): e0235891. https://doi.org/10.1371/journal.pone.0235891

[2] Budd C., Calvert K., Johnson S. and Tickle S. O. 2021Assessing risk in the retail environment during the COVID-19 pandemic. R. Soc. open sci.8210344. 210344 https://doi.org/10.1098/rsos.210344

4 Outside & Unticketed

For this section we consider as inspiration the use case of the Edinburgh Fringe as it has many of the characteristics of an unticketed, outdoor event. The Edinburgh Fringe is a three-week festival, the Fringe itself is a small organisation, a loose affiliation of independent promoters. Outdoor street performances form a major part of the attraction to the Fringe - in a typical year, there might be 130 street performers, 1,200 slots and 400 buskers in 50,000 slots, plus a similar number of promos etc. - they are however an uncontrolled part of event. These street performers are un-managed insofar as there is only loose management, with a limited number of stewards.

Given the pandemic, in 2021 will be some modifications. There will be fewer acts (no internationals) - perhaps 20 % reduction. There is an unknown COVID19 hesitancy in the crowd (mask wearing; some high spirits "freedom day"). There will be a cashless money collection principle. As of the beginning of the festival, all rules national rules are likely to have been relaxed, only guidelines to be issued. The police / council will seek control, but if street performers are banned, they will happen anyway with less control.

A key question for this group to address is **what guidelines will help maintain COVID19 safety? How can they be applied?**

4.0.1 Key aspects of the problem

- both the performers and the crowd are uncontrolled

- unpredictable numbers and new untested environment (e.g. outside bars)

- no one really knows the state of COVID19 spread and vaccination status

- unlikely to be any controlled track, test and trace

- crowd may not respond to nudges and cues from stewards

- performers are likely to fill a space if they see it with unexpected "pop-ups"

- performers can be agents of control; will listen to stewards (5 minutes to go etc.) within limits; but could be agents of rebellion.

- with appropriate science / messaging / negotiation maybe compromise on time (< 45 mins) or crowd size can be reached

- will physical crowd management (one-way systems etc) help or hinder?

In this context **when does an un-managed crowd become a public health when there is some underlying contagion (COVID19) in circulation?**

4.0.2 Initial ideas for mitigation strategies

There are manual and guidance which are industry standards by which organisers should run large events [SOME REFS]. These however generally don't apply to the Fringe example as they assume some level of command and control. The organic, devolved authority use case of complex free agents is less well studied. However, the general principle of **design, information & management** [REF] do apply. In this instance, the group is looking to provide probable solutions, not optimised answers. The key assumption is that we can use the street performers as agents of (subliminal) control for example:

- provide directions from the stage (move back, move forward, stop now etc.)

- the **Pink Policemen** - instead of stewards have people in pink with squeaky truncheons to support control, but with an element of performance - or **Sanitiser Fairies**

- use of "pied pipers" as leaders of crowd to less crowded spaces

How to quantify risk of person-to-person infection to make guidance seems to be the most important thing to consider; how do we know when there's a mix of infectious and susceptible people, how does the transmission behave.

4.0.3 Quantitative modelling

All evidence points to airborne infection as dominant transmission route for COVID19, which increases in a festival environment due to singing, laughing etc. This section makes the working assumption that brief interaction outdoors are OK, but we want to avoid static gatherings for too long, too close. To begin to quantify this we assume that we don't know vaccination status of everyone, and that there will be plenty of susceptibility within the crowd; as such we have ignored vaccinated people in the crowd (considered as inert people who maje the crowd larger), and also have not included the impact of test & trace. This section focuses on the following modelling topics:

1. person-to-person modelling - probability of one infectious person infecting

2. small crowd modelling - how many will they infect during 1 street performance

3. people flow modelling - how to avoid log-jams that will lead to dense crowds

4.1 Can we estimate the person-to-person transmission probability outdoors?

Ref. [10] model 'quanta of infection' Q from one infected person. $Q = 1$ is viral dose inhaled that gives 65% probability of infection. ER_q is expiration rate of quanta (per hour)

$$ER_q = c_i c_v IR n_q; \quad n_q = \sum_{\text{particles } i=1}^{4} V_i N_i$$

where IR is inspiration rate, $c_{i,v}$ viral load to infection conversion factors. From data we obtain $n_{\text{out}}^{\text{breathing}} = 0.0442, \quad n_{\text{out}}^{\text{laughing}} = 1.12$, hence

$$ER_q^{\text{breathing}} \sim 1 - 100, \quad ER^{\text{laughing}} \sim 25 - 2500$$

but Q is number not density and ER_q is number/hour

Simplified person-to-person infection model

This then enables you to perform some back of the envelope diffusion type modelling on how does that dissipate, assuming a $1/r^2$, and linear in time behaviour. For stationary conditions

$$Q \sim ftg(r) \tag{11}$$

We take $f \in [1, 400]$ and

$$g(r) = \begin{cases} 1 & \text{if} \quad r < n \\ \frac{1}{r^2} & \text{if} \quad n \le r \le m \\ 0 & \text{if} \quad r > m \end{cases}$$

For our purposes,

$$n = 1 \quad \text{and} \quad m = 5.$$
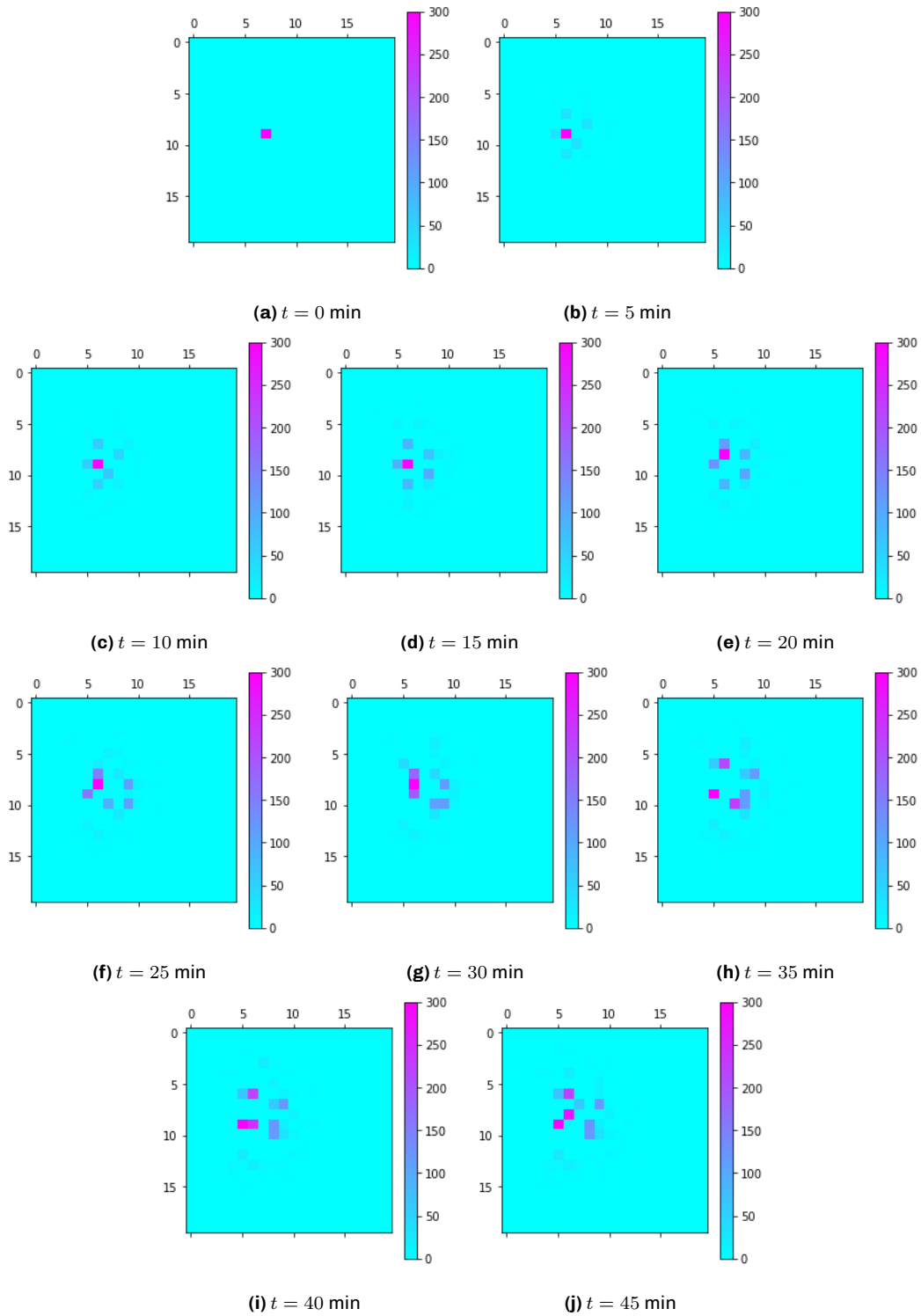
Caveats / future work

- Note $1/r^2$ comes from spray-like assumption of constant velocity expiration

- Note if diffusion dominated variation will behave as $1/r$ for steady case

- Appropriate modification can be made for unsteady cases (solving the diffusion equation), in wind (allowing for convection) and multiple sources of viral quanta.

- f represents the production rate of quanta over velocity of the spray and account can be taken as directionality of the spray.

- Effect of droplets landing on eyes, skin etc. ignored.

- We have ignored wind and other atmospheric sources of convection, Ref. [11]

4.2 Can we quantify the risk amongst a crowd watching a performer?

We are going to consider a lattice based model which is discrete in time and space. The model considers a 10m×10m square with shortest distance between two people 0.5m, and time evolves as $t = 5, 10, 15, \ldots 45$ mins. Each person can change location within a square around them. We consider the case where 1 infectious person among ~ 179 susceptible people in the audience (taking into account some probability of infectiousness). The probability that you want to move to an adjacent square in a particular timestep is 0.5. We use (11) to calculate the viral quanta Q received by each individual and probability of infection.

In Fig. 22, an example run is shown, the infectious person is shown as the purple square, they are not wearing a mask and they are signing the entire time.

(a) $t = 0$ min

(b) $t = 5$ min

(c) $t = 10$ min

(d) $t = 15$ min

(e) $t = 20$ min

(f) $t = 25$ min

(g) $t = 30$ min

(h) $t = 35$ min

(i) $t = 40$ min

(j) $t = 45$ min

Figure 22: Example run with an infectious person that doesn't wear a mask in a 45-minutes event, and sings (or laughs) all of the time.

Preliminary conclusions

The model is run by a Monte Carlo approach and averages to make the following preliminary conclusions.

- Effect of infected person wearing a mask

$$41(23.0\%) \mapsto 14(7.8\%) \quad 2.9 \times \text{decrease})$$

- Effect of people singing for entire 45 minute duration

$$41(23.0\%) \mapsto 70(39.0\%) \quad (1.7 \times \text{increase})$$

- Effect of reducing performances from 45 minutes to 25 minutes, assuming the infectious person sings the entire time.

$$70(39\%) \mapsto 66(37\%) \quad (1.06 \times \text{decrease})$$

Conclusion: wear a mask while standing to watch a performance is most effective measure rather than cutting show time, can this be used as incentive and built into the performance?

4.3   Can we model crowd behaviour? Including bottlenecks, density, followers and leaders?

The goal in this section is to model crowd dynamics; how do pedestrians walk around the city, so to investigate this problem the group used an off-lattice individual based model (IBM). The group considered two geometries; Edinburgh city streets and a hypothetical street map. It is assumed that individuals are guided by directional cues (e.g. gradient, buildings or following a leader) or they don't find an directional cue, they move randomly. Using these models, the group looked to address the following questions:

- How is crowd density affected by social distancing and width of roads?

- How do obstacles change pedestrian flow?

- If a venue attracting pedestrians is introduced to the model, what happens?
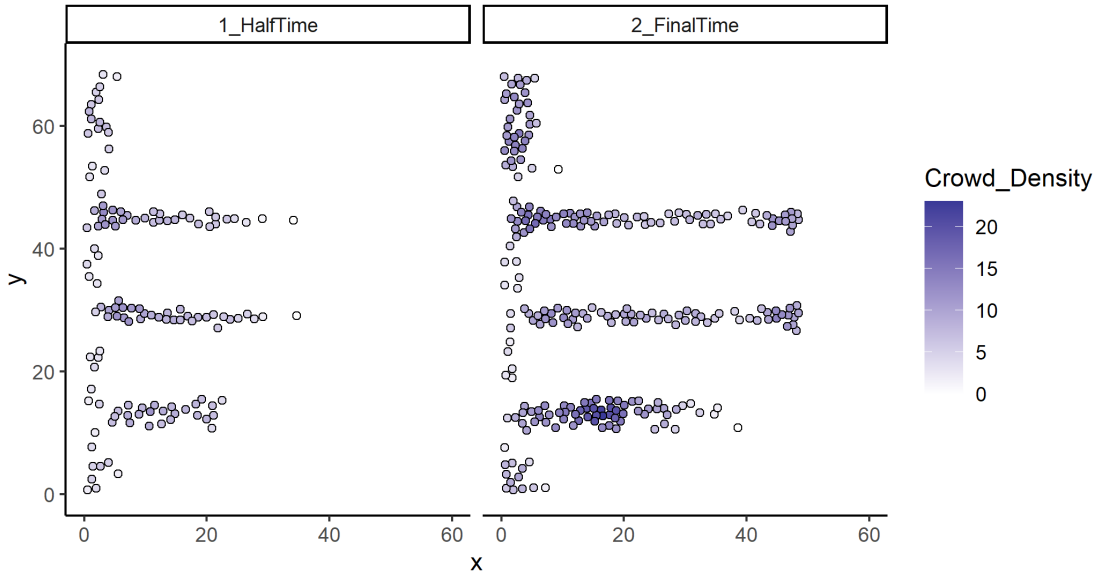
Figure 23: Three roads 1 m social distance, 5 m road width crowd density of agents.

Control case: Fig. 23 shows a simulation with three roads, of differing gradients. For all the simulations shown here, the left panel is a half-time snapshot and the right panel is the full time situation.

Increased Social Distancing: Fig. 24 enforces a social distance on top of the control scenario, and shows the density of the crowd.
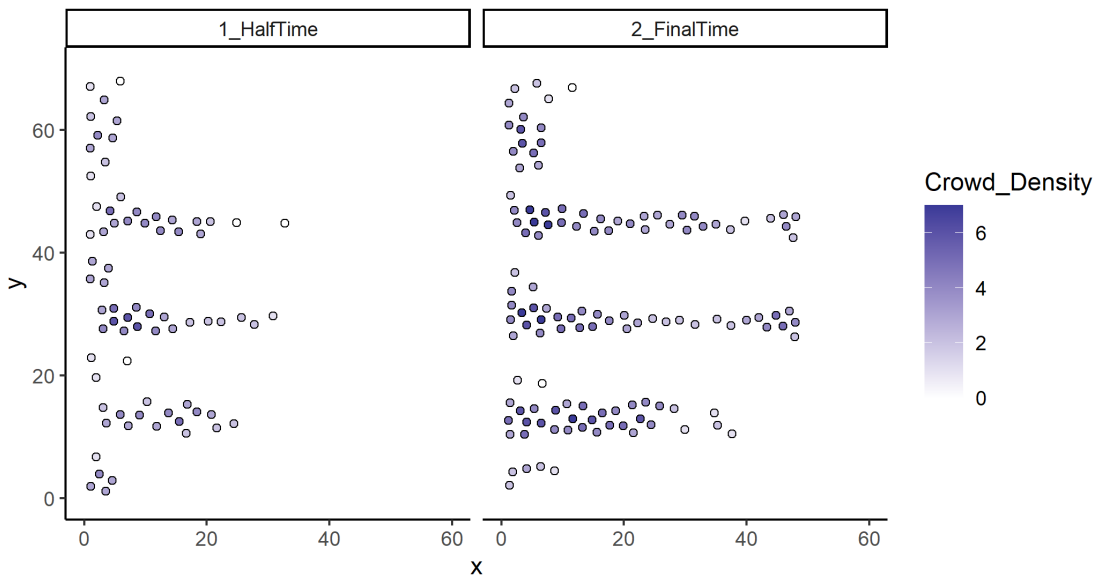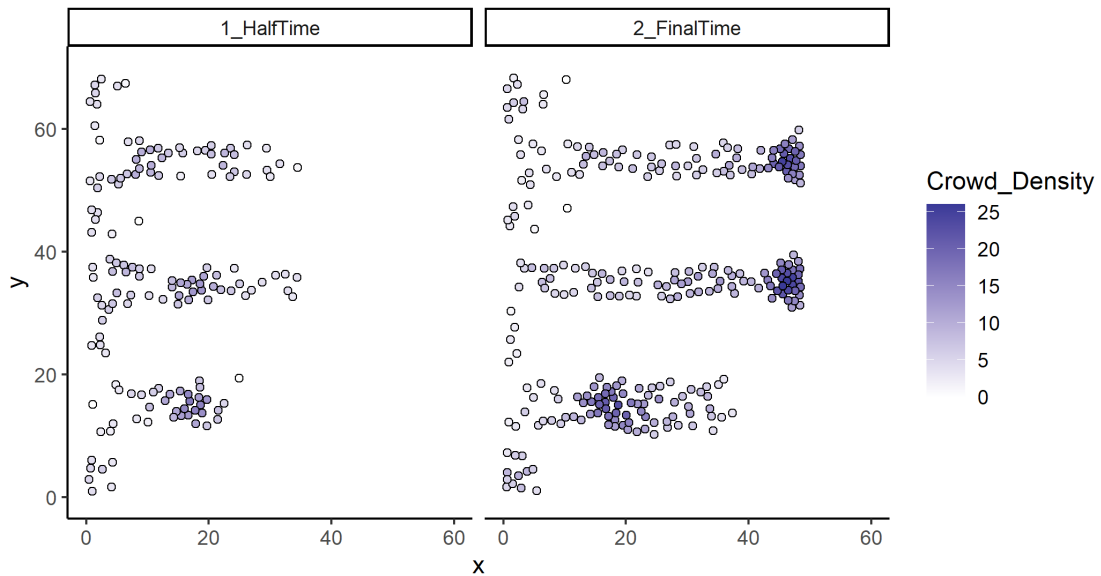
Figure 24: Three roads 2 m social distance, 5 m road width crowd density of agents.

Introducing an Obstacle: Fig. 25 shows the results of a simulation where an obstacle is introduces (at around 20 m); this could correspond to a street performer setting up, or a marshal asking people to slow down.
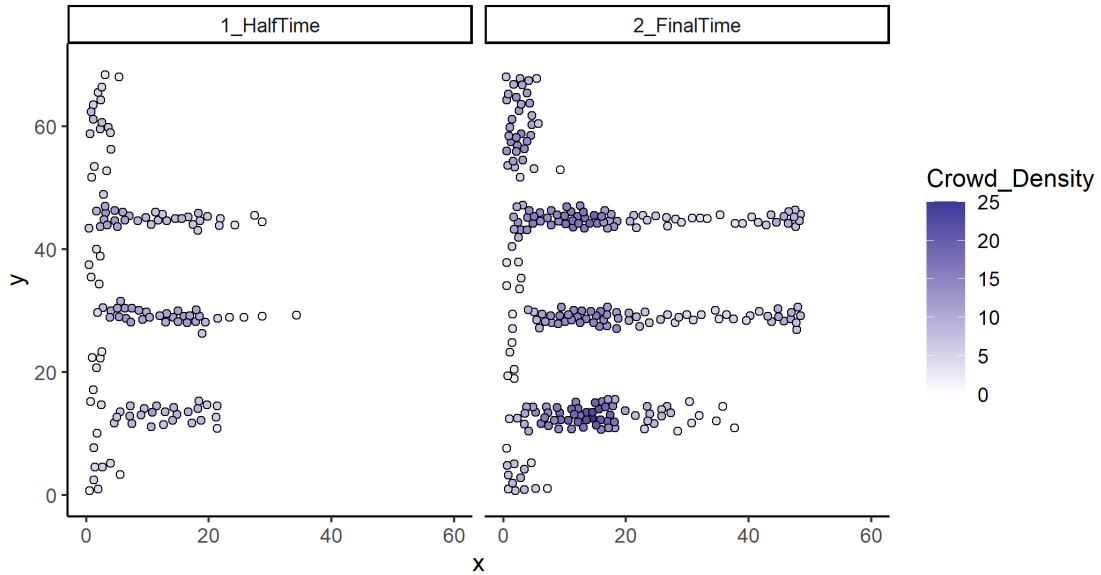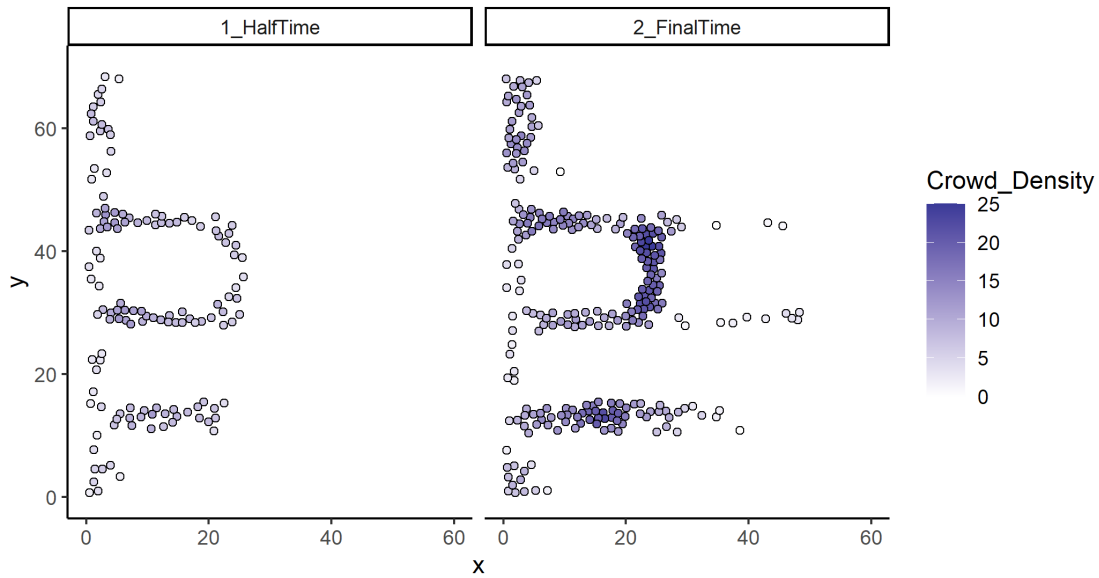

Figure 25: Obstacle and three roads 1 m social distance, 5 m road width crowd density of agents.

Increasing Road Width: Fig. 26 shows the effect of increasing the road width on the crowd density.

Figure 26: Three roads 1 m social distance, 10 m road width crowd density of agents.

Adding a Venue in between two roads: Fig. 27 shows the impact of introducing an avenue between two of the roads.

Figure 27: Popular spot with three roads 1 m social distance, 5 m road width crowd density of agents.

Summary statistics

Table 4: Model 2 - increased social distancing; Model 3 - an obstacle in the middle of the roads; Model 4 - increasing road width; Model 5 - adding a popular venue in between the roads.

	Number of agents	Crowd density
Control	258	10
Model 2	125	4
Model 3	258	11
Model 4	280	9
Model 5	258	12

Modelling Edinburgh streets: redirecting people: In this section, we demonstrate the feasibility of using pre-existing tools to demonstrate relative impact. Fig. 28 (left) shows an example where lots of people are missing about, and we model the scenario of one group wanting to move left-to-right and the other group wanting to move right-to-left.

Fig. 28 (right) shows what might happen if there is a person or very effective signage which encourages people to change their direction. We might consider that 20 % are diverted to the south-side of the map. These simulation are relatively simple and quick to put together.
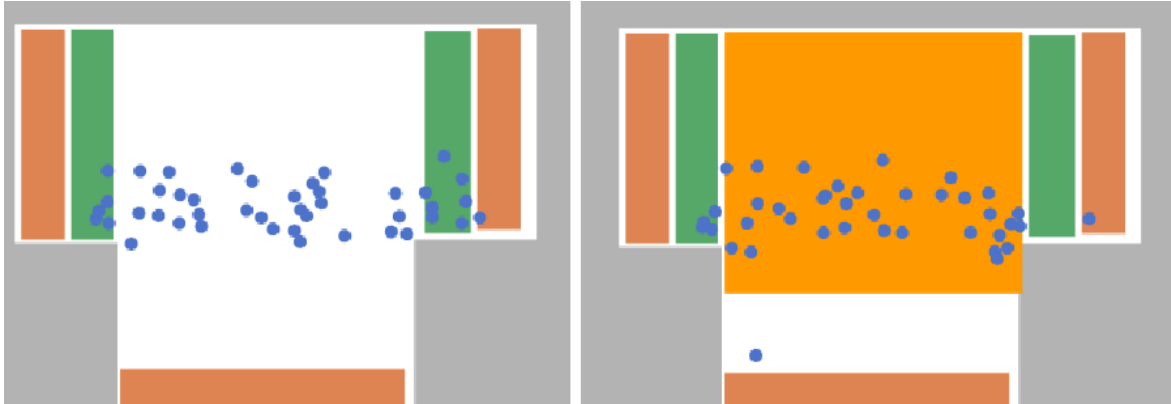
Figure 28: (left) agents moving from red to green (right) orange area in the middle has a probability of diverting those agents southwards.

Fig. 29, we can look at how many people are coming within 2 m of each other, and look at the effect of (a) no redirection, (b) 20% redirection and (c) 40% redirection and we can see that change in the mean value and the relative impact.
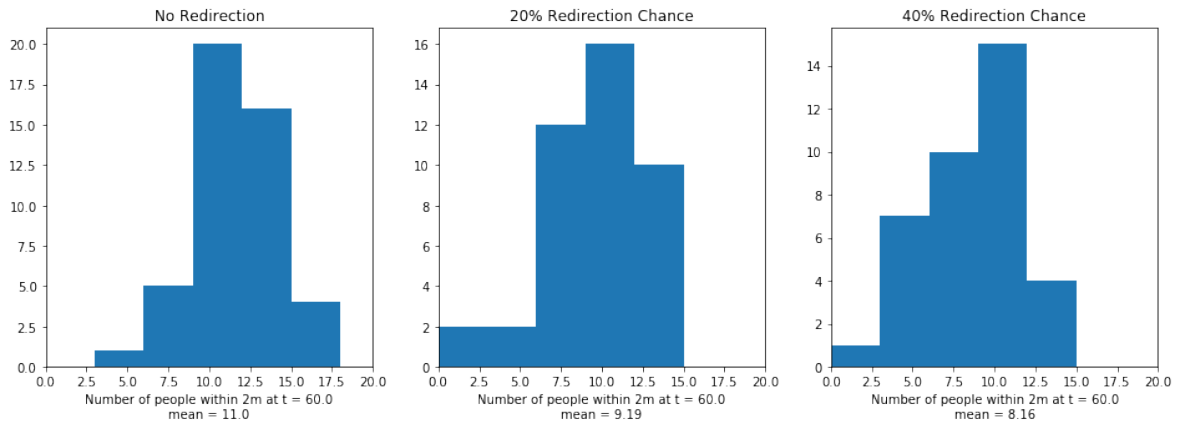
Figure 29: Histograms demonstrating the impact of redirection on proximity of agents.

Hunter Square Obstruction: In Fig. 30 we are modelling a specific part of Edinburgh - the idea is you have lots of people in the cathedral area and someone sets up in one of the side-streets that people will want to move through, and so we can look at what if it is (a) an obstruction people can walk around or (b) an attraction that cause people to stand around and watch / listen.

In Fig. 30 (middle) there is a small grey area - the obstruction. In Fig. 30 (right) anyone that

moves into orange area they have a small chance (20 %) that they'll hang around and listen to the performer.

Figure 30: Cathedral area of Edinburgh, comparison of (left) no side street obstruction (control) (middle) obstruction on the side street and (right) attraction on the side street.

Once again, Fig. 31 is a histogram of the relative effect on agent proximity of the above scenarios. The effect of putting an obstruction there isn't really much change at all above the control, but if there is an attraction which makes people want to hang around and listen, then actually we see a lot more grouping up even amongst those who are not standing around to listen.
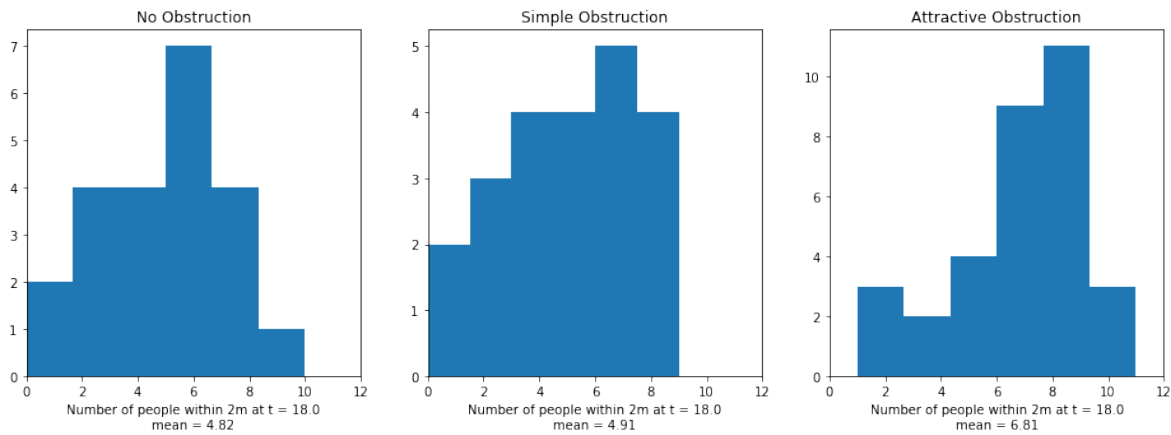
Figure 31: Histograms demonstrating the impact of redirection / attraction on proximity of agents.

Conclusions of crowd modelling:

- This kind of modelling may allow us to assess the relative impact of interventions / measures designed affect how people move around events.

- (arguably) better to use this kind of modelling than bespoke crowd modelling software

because of the degree of crowd uncertainty

- Redirection (the pied piper effect) can help reduce the largest density bottle-necks

4.4   Conclusions & future work

The complexity and free agency of crowds means this is **not** an optimisation problem, but one of **risk mitigation strategies**. The working assumption throughout our modelling us that infection risks occur when people gather relatively statically without masks.

Can we estimate the person-to-person transmission probability outdoors??

- here we derive an approximation which provides a 'quanta of infection', this derivation allows for simple, diffusion type modelling on how virus dissipates for use in the following sections.

- in quantifying the risks, we suggest risk increases linearly with exposure time and that risk is multiplied by factor 25 if singing or laughing - particularly important considering event types.

Can we quantify the risk amongst a crowd watching a performer?

- We use a lattice based model to simulate movement of individuals in an open space over time whilst watching a street performer. The relative impact of wearing a mask in an audience compared with shortening the show is considered. A tentative conclusion is that mask wearing during a performance is the most effective measure to reduce risk.

- it is suggested that controlling the behaviour of static crowds (by performers encouraging **mask wearing** in their audience) could be a valuable risk mitigation strategy.

- Further work should consider:

  - how passers-by past and / or through crowds watching performers might impact transmission risk.

  - Modelling motion of audience between and beside acts

  - Consideration of motion within a crowd, e.g. trying to get a better view, or avoid reach of the performer

  - If performer indicates good idea for some audience to leave; who will go? People who've been there longest (probably near the front?) or those near the back (easy to get away and without good view)?

- – The effects of people 'barriers' protecting people behind them

- – Effects of wind and directionality for spray of viral load

- – Current mathematical model effectively reduces to $P(\text{infection}) = 1 - \exp(-At/r^2)$ where A is an unknown dependent on factors like spread and propulsion of droplets. Can we ignore all these factors and just fit A to data?

- – Vaccinated individuals, people with or without masks, distribution of strengths of sources amongst infected people (a few might be "super spreaders"), how to use some knowledge of recent infect rates.

Can we model crowd behaviour? Including bottlenecks, density, followers and leaders?

- Here we consider how dynamic crowd interventions (such as redirection) could be used to minimise congestion of crowds (therefore infection risk). We suggest redirection (possibly using 'pink police' as **pied pipers** as part of a performance) could be a valuable method for reducing risky transmission events.

- Future work would need to consider a more sophisticated behavioural understanding of these crowds

References

[1] Thompson, H. A. *et al* Report 38: SARS-CoV-2 setting-specific transmission rates: a systematic review and meta-analysis. `https://www.imperial.ac.uk/media/imperial-college/medicine/mrc-gida/2020-11-27-COVID19-Report-38.pdf`

[2] Agrawal, A., & Bhardwaj, R. (2021). Probability of COVID-19 infection by cough of a normal person and a super-spreader. Physics of fluids (Woodbury, N.Y. : 1994), 33(3), 031704. `https://doi.org/10.1063/5.0041596`

[3] E. C. Riley, G. Murphy, R. L. Riley, Airborne spred of measles in a suburban elementary school, American Journal of Epidemiology, Volume 107, Issue 5, May 1978, Pages 421–432, `https://doi.org/10.1093/oxfordjournals.aje.a112560`

[4] Sze To, G. N., & Chao, C. Y. (2010). Review and comparison between the Wells-Riley and dose-response approaches to risk assessment of infectious respiratory diseases. Indoor air, 20(1), 2–16. `https://doi.org/10.1111/j.1600-0668.2009.00621.x`

[5] Bhagat, R., Davies Wykes, M., Dalziel, S., & Linden, P. (2020). Effects of ventilation on the indoor spread of COVID-19. Journal of Fluid Mechanics, 903, F1. doi:10.1017/jfm.2020.720

[6] Budd C., Calvert K., Johnson S. and Tickle S. O. 2021Assessing risk in the retail environment during the COVID-19 pandemic. R. Soc. open sci.8210344. 210344 `https://doi.org/10.1098/rsos.210344`

[7] Setti, L., Passarini, F., De Gennaro, G., Barbieri, P., Perrone, M. G., Borelli, M., Palmisani, J., Di Gilio, A., Piscitelli, P., & Miani, A. (2020). Airborne Transmission Route of COVID-19: Why 2 Meters/6 Feet of Inter-Personal Distance Could Not Be Enough. International journal of environmental research and public health, 17(8), 2932. `https://doi.org/10.3390/ijerph17082932`

[8] Belosi, F., Conte, M., Gianelle, V., Santachiara, G., & Contini, D. (2021). On the concentration of SARS-CoV-2 in outdoor air and the interaction with pre-existing atmospheric particles. Environmental research, 193, 110603. `https://doi.org/10.1016/j.envres.2020.110603`

[9] Johansson, A., Batty, M., Hayashi, K., Al Bar, O., Marcozzi, D., & Memish, Z. A., (2012). Crowd and environmental management during mass gatherings The Lancet Infectious Diseases, 12, 2, p150. `https://doi.org/10.1016/S1473-3099(11)70287-0`

[10] Buonanno, G., Stabile, L., & Morawska, L. (2020). Estimation of airborne viral emission: Quanta emission rate of SARS-CoV-2 for infection risk assessment. Environment international, 141, 105794. `https://doi.org/10.1016/j.envint.2020.105794`

[11] B.R. Rowe, A. Canosa, J.M. Drouffe, J.B.A. Mitchell, Simple quantitative assessment of the outdoor versus indoor airborne transmission of viruses and COVID-19, Environmental Research, Volume 198, 2021, 111189, ISSN 0013-9351, `https://doi.org/10.1016/j.envres.2021.111189`

[12] Joana Margarida de Almeida Simoes. An agent-based approach to spatial epidemics through GIS (2006). University College London. `http://www.casa.ucl.ac.uk/JoanaMargarida/thesis_post_viva.pdf`

[13] Briers, M., Charalambides, M., & Holmes, C. Risk scoring calculation for the current NHSx contact tracing app `https://arxiv.org/pdf/2005.11057.pdf`

[14] Gammaitoni, L., & Nucci, M. C. (1997). Using a mathematical model to evaluate the efficacy of TB control measures. Emerging infectious diseases, 3(3), 335–342. `https://doi.org/10.3201/eid0303.970310`

[15] Bazant, M. Z., and Bush, J. W. M. A guideline to limit indoor airborne transmission of COVID-19. PNAS April 27, 2021 118 (17) e2018995118; `https://doi.org/10.1073/pnas.2018995118`

5   List of Acronyms

EQ emission quanta

IBM individual based model

ICMS International Centre for Mathematical Sciences

LFD lateral flow device

LFT lateral flow test

ODE ordinary differential equation

PPL probabilistic programming language

qPCR quantitative polymerase chain reaction

RNA ribonucleic acid

VSG Virtual Study Group

ICMS
The Bayes Centre,
47 Potterrow Upper Street
Edinburgh, EH8 9BT

Email: info@icms.org.uk
icms.org.uk
@ICMS_Edinburgh

Contact Person
Dawn Wasley
dawn.wasley@icms.org.uk